

The down sign NOTIFY that the present project with the title:

Behavior Study of Pipes after Forming, Coating and Bending

and determined for Jordi Marquez Llinás by eligibility for the qualification of the Degree in Materials Engineering in Universitat Autònoma de Barcelona, has been made under the university management being all the results and procedures in the present documentation done for the above mentioned.

For this purpose, the present certificate is signed by:

PHd. Baró M.D
Head of Materials Physics II Department
Universitat Autònoma de Barcelona

Acknowledgements

It is my sincerely wish to dedicate this project without any order of importance to:

My parents and part of the family, especially my cousin Ramon and Ana for all the truly and unconditional love and support to my person in the good and not so good moments.

Moi my childhood friend for all these years by my side offering me always the best of himself.

Núria to change much of my life and for all the love and understanding towards me.

Edu for the unconditional and sincerely help and support both in Spain and Belgium and all the good moments lived always.

Cristiane for returning to the faith in many things and offer me the best of yourself sincerely and selflessly.

Dolors Baró, to trust in me allowing and opening this quite desired way to do this project abroad.

OCAS for giving me the opportunity of these 6 months of internship.

CFGS my Sabadell teachers, especially Santandreu and Rafa, infusing me new hopes for returning to finish my studies and career.

Tania and Carlos for their support and patience in some really bad moments.

Marga and Pau for your sincerity and all the entire conversations and great moments shared.

And in memory of my aunt, Luisa, who taught me so much offering the best of herself without asking anything in return, with her best smile, happiness and energy.

Gratefully thanks to all of you with my whole heart.

Table of Contents

1 INTRODUCTION5

1.1 HISTORY OF PIPELINES..... 5

1.2 PIPELINES LOCATIONS AND ENVIRONMENTS..... 6

1.3 PROCEDURES OF PIPELINES MANUFACTURING 7

1.3.1 SEAMLESS7

1.3.2 LONGITUDINALLY WELDING USING ELECTRICAL RESISTANCE WELDING (ERW).....8

1.3.3 LONGITUDINALLY WELDING USING SUBMERGED ARC WELDING (SAW).....9

1.3.4 HELICAL OR SPIRAL WELDED 11

1.4 PIPELINES STEELS..... 11

1.5 PIPELINES COATINGS 15

2 JUSTIFICATION AND OBJECTIVES.....16

3 EXPERIMENTAL METHODOLOGY17

3.1 SAMPLING AND COATING RECREATION..... 17

3.2 TENSILE TEST..... 18

3.2.1 MECHANICAL PROPERTIES19

3.2.2 EXPERIMENTAL TENSILE TEST DESCRIPTION23

3.3 HEAT TRANSFERS IN CHARPY V-NOTCH 24

3.3.1 ENERGY TRANSFER24

3.3.2 ANALYTICAL DESCRIPTION.....27

3.3.3 EXPERIMENTAL HEAT TRANSFER CHARPY V-NOTCH PROCEDURE.....33

3.4 CHARPY V-NOTCH IMPACT TEST..... 35

3.4.1 CHARPY TEST METHOD..... 36

3.4.2 MECHANICAL FRACTURES AND DBTT IN CHARPY37

3.4.3 EXPERIMENTAL CHARPY V-NOTCH PROCEDURE39

3.5	<i>FEM SIMULATION</i>	41
3.5.1	GENERAL SIMULATION STRUCTURE STUDY CASE	41
3.5.2	PREPROCESSING AND MODEL SET-UP.....	47
4	RESULTS AND DISCUSSION	60
4.1	<i>SAMPLING AND COATING RECREATION</i>	60
4.2	<i>TENSILE TEST</i>	61
4.3	<i>HEAT TRANSFERS IN CHARPY V_NOTCH TEST</i>	66
4.3.1	ANALYTICAL PROCEDURE	66
4.3.2	EXPERIMENTAL PROCEDURE	72
4.4	<i>CHARPY V-NOTCH IMPACT TEST</i>	74
4.5	<i>FEM SIMULATION</i>	77
5	CONCLUSIONS	81
6	FUTURE WORKS.....	82
7	ENVIRONMENTAL ASPECTS	82
8	COSTS.....	83
9	REFERENCES.....	85

1 INTRODUCTION

1.1 HISTORY OF PIPELINES

The first pipeline was built in the United States in 1859 for the transport of the crude oil ^[1]. Through the one-and-a-half century of pipeline operating services, the petroleum industry, which has been acquiring each year more importance, has proven that pipelines are by far the most economical means of large scale overland transportation for crude oil, natural gas, and their products versus rail, ship and truck transportation.

According to the industrialization age, these types of products to obtain energy are demanded in more large quantities to be moved on a regular basis, being this differences more clear every year.

Due to the transport of petroleum fluids with pipelines is a continuous and reliable operation, and the ability to adapt to a wide variety of environments such remotes areas, hostile environments, etc. the use of pipelines have been increased and nowadays, are used to connect countries and continents with the areas where is extracted and the refineries so offshore pipelines can be classified as follows (*Figure 1.1*):

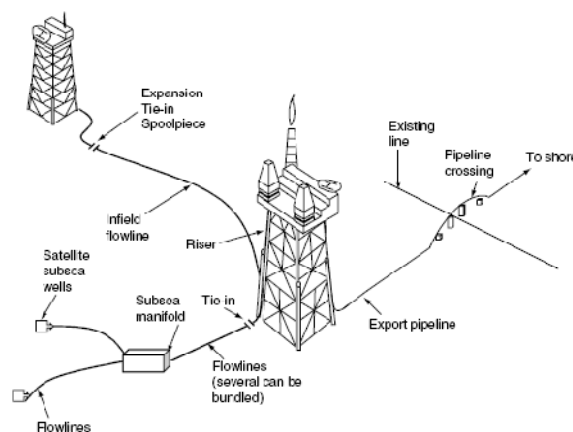


Fig.1.1 – Offshore subsea pipeline use

- Flowlines transporting oil and/or gas from satellite subsea Wells to subsea manifolds.
- Flowlines transporting oil and/or gas from subsea manifolds to production facility platforms.
- Infield Flowlines transporting oil and/or gas between production facility platforms to shore.
- Flowlines transporting water or chemicals from production facility platforms through subsea injection manifolds to injection wellheads.
- Flowlines transporting oil and/or gas from shore to refineries to be treated and distributed.

1.2 PIPELINES LOCATIONS AND ENVIRONMENTS

Nowadays, exist a global worldwide wire of pipelines for the crude distribution around the world, in fact, usually the oil fields are placed so far from the consumption areas. In example, Occidental Europe exports 97% of its necessities mainly from Africa or Western Asia (Figure 1.2). Other countries such Russia, EEUU, Canada, etc., also need to export crude oil from very far regions.



Fig. 1.2 – European and Western Asia crude oil and gas pipelines connection

Each earth region, has specific environmental conditions and also quite different geography conditions, from the crude source to final destination so the needed locations of the pipelines routes have to be adapted according the geography and land possibilities as well the most beneficial economical factors. Different locations are shown below (Figure 1.3 a, b, & c):



Fig. 1.3 – a) Extreme cold environment(Alaska)

b)Moderate environment
Arabia)

c)Extreme hot environment (Desert of

1.3 PROCEDURES OF PIPELINES MANUFACTURING

Nowadays, for oil and gas industry, the pipes are commonly made by one of following four fabrication procedures ^[2]:

1.3.1 SEAMLESS

Seamless pipe is formed by hot working steel to form a pipe without a welded seam. This procedure can be done by different ways.

The initially formed pipe may be subsequently cold worked to obtain the required diameter and wall thickness and after heat treated to modify the mechanical properties. To obtain the pipe, a solid steel bar is firstly drilled from a slab and is subsequently heated and formed by rollers around a piercer to produce the length of the pipe (*Figure 1.4*).



Fig. 1.4 – Seamless pipe process

The main disadvantages of this procedure are: higher costs to obtain in comparison with alternative procedures, although the process is quite slow (rollers usually turning between 100-150RPM in function of diameter), other disadvantages are a fairly wide variation of wall thickness (around 15%) and out of roundness and straightness.

1.3.2 LONGITUDINALLY WELDING USING ELECTRICAL RESISTANCE WELDING (ERW)

ERW pipe is formed from coiled plate steel. The plate is uncoiled and sheared to the required width, flattened and the edges are dressed. The plate is passed through a sequence of rolls to form the pipe, crimping the edges of the plate and then progressively bending the plate into a circular final form, ready for welding in the longitudinal direction (*Figure 1.5*):

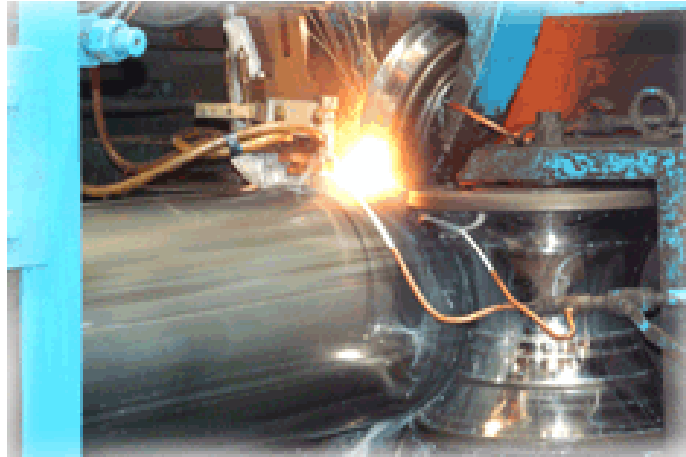


Fig. 1.5 – ERW Process

The welding step, consist on applying electrical current across the interface of the steel pipe needed to be heated for welding, obtaining a heating in both pipe faces to be welded. Once heated the faces are pressed together to produce the longitudinal seam weld using induction coils operating at low frequency (60-360Hz of AC) or induced into the steel with induction coils operating at high frequencies of above 400KHz, termed High Frequency Induced (HFI) ERW procedure.

HFI, is commonly used for submarine pipelines due to HAZ (*Heat Affected Zone*) is slower than the other methods, because of the electrons that carry the current tend to flow increasingly at the outer surface of the conductor and at high frequencies the electron movement is exclusively in the outer 1mm or less of the conductor, allowing to the pipe walls to melt in a very small area long to longitudinal direction.

1.3.3 LONGITUDINALLY WELDING USING SUBMERGED ARC WELDING (SAW)

The pipe is formed from individual plates of steel and subsequently applying 4 steps once the plate is trimmed. For the forming steps it is also commonly named, U-O-E process ^[3].

- **FIRST STEP**

First forming step involves crimping of the edges of the plate into circular arcs over a width of about one radius on each side pressing the ends between two shaped dies applying it in several steps due to the high pressure that is needed (*Figure 1.6*):

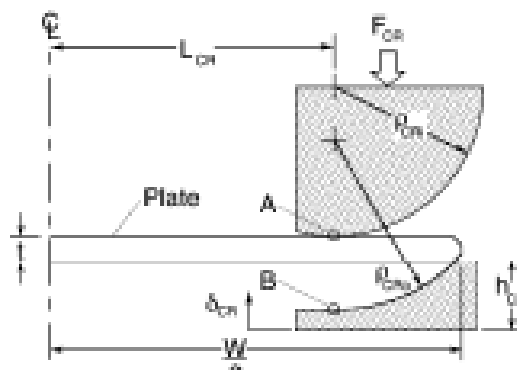


Fig. 1.6 – First step forming

- **SECOND STEP FORMING**

On second step forming process the plate moves to U-press where centered the U-punch moves down and bends the entire plate through three-point bending. The U-punch is held in place and the side rollers are moved inwards (*Figure 1.7*):

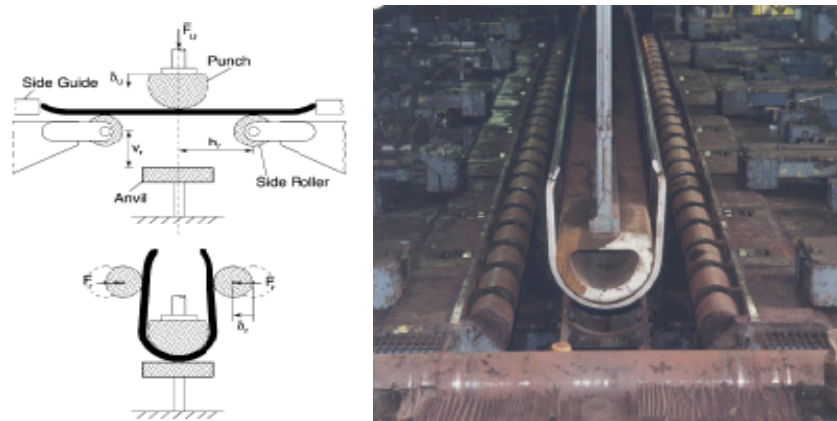


Fig. 1.7 – Second forming process

- **THIRD FORMING STEP**

In the third forming step, the skelp is then conveyed to the O-press consisting of two semi-circular stiff dies (*Figure 1.8*). The top die is actuated downwards forcing the skelp into a nearly circular shape.

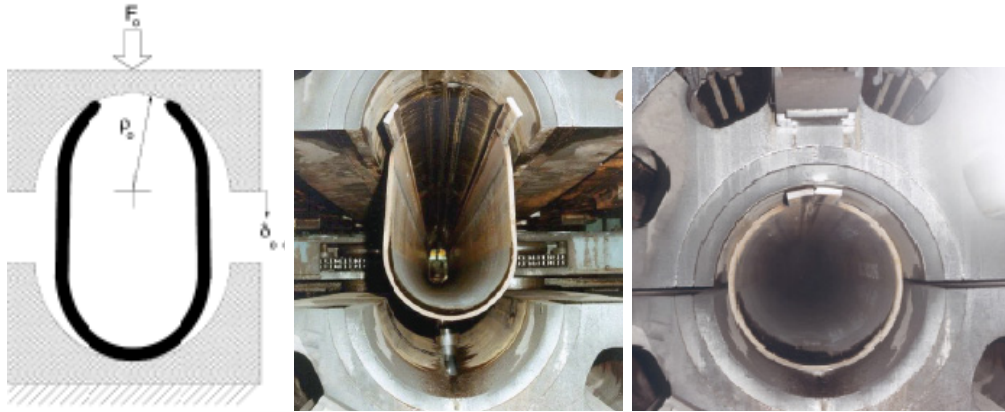


Fig. 1.8 – Third forming process

- **FOURTH FORMING STEP**

On this step the skelp is welded and a final expansion step is accomplished by an internal mandrel achieving low ovality due that the pipe is expanded from 0.8 to 1.3% from its diameter after the O-step (*Figure 1.9*):

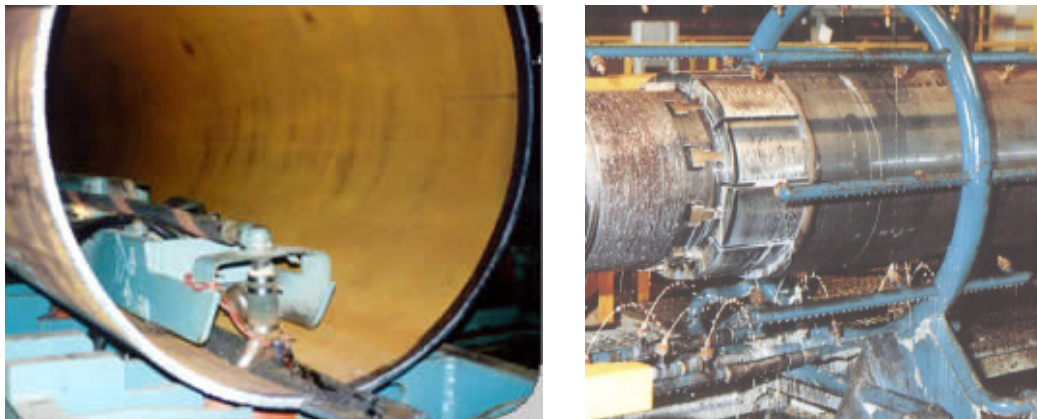


Fig. 1.9 – a) SAW Longitudinal Welding

b) Fourth forming Expansion step

1.3.4 HELICAL OR SPIRAL WELDED

For this procedure, a coil of hot-coiled plate is uncoiled, straightened, flattened and edges dressed. Then the plate is helical wound to form a pipe which its diameter depends of the width of the strip and the angle of coiling. Once is formed, the helical internal seam is welded using SAW or inert gas, and as the seam rotates to the top position, the external weld is made (*Figure 1.10*), obtaining a continuous length of pipe which is passed through a sequence of rollers to enhance circularity. Finally the pipe is tested using radiography or ultrasonic testing and finally cutted to the required lengths.

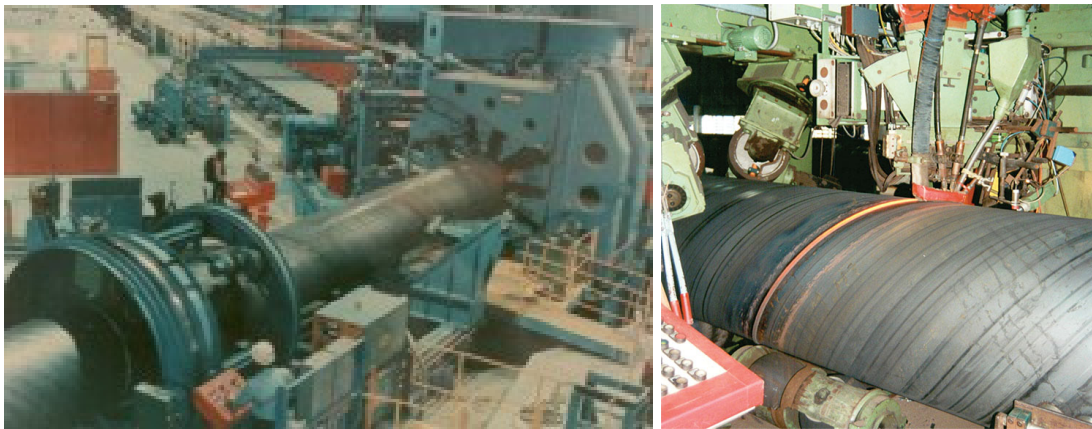


Fig. 1.10 – Spiral Welded Pipe Process

1.4 PIPELINES STEELS

Pipeline steel must have high strength while retaining ductility, fracture toughness and weldability^{[1][4]}.

- **Strength** is the ability of the pipe steel and the associated welds, to resist longitudinal and transverse tensile forces imposed on the pipe in service and during installation.
- **Ductility** is the ability of the pipe to absorb overstressing by deformation.
- **Toughness** is the ability of the pipe material to withstand impacts or shock loads and the behavior of the material is very important, indeed, brittle or ductile fracture manner.
- **Weldability** is the ability and ease of production of a quality weld with an adequate strength and toughness in the HAZ.

The balance of properties (*strength, toughness and weldability*) required depends on the intended use of the pipeline. Due to the increasingly energetic demand in last decades, since mid 1960s, the requirements become more exigent and also the transport reduction costs. For these reasons more standards (*regulated by API, American Petroleum Institute, ASME, American Society of Mechanical Engineers, ISO, International Standards Organization, etc...*) have been developed to standardize the entire pipelines world.

Due to the higher operating pressures the diameter of the pipes was increased and also in service requirement. For this purposes thicker wall pipes were needed.

The primary design parameter for this effort is the Yield Strength (YS) because as the YS increases, the wall thickness requirement decreases. It is needed to take into account also the environmental effects, pipe manufacturing procedures, the type of fluids and the in service operating conditions.

Engineering materials have four essential characteristics that are closely interrelated:

- Chemistry: The primary element (*Fe*), alloying elements (*Ni, Cr, etc. with ferrous metals*), unintended elements and impurities of other elements.
- Physical properties: Density, modulus of elasticity, coefficient of thermal expansion, electrical and heat conduction, etc.
- Microstructure: Atomic structure, metallurgical phases, type and size of grains.
- Mechanical properties: YS (*ultimate elongation at rupture*), toughness (*Charpy nil ductility transition temperature, fracture toughness*).

The materials used in pipelines systems can be classified in two large categories: metallic and non-metallic. Focusing on metallic exist also two internal categories: ferrous (*Fe based*) or non-ferrous (*Cu, Ni or Al based*).

Nowadays, the most widely steel grades used are x65, x70, x80 and x100. This project is focused only in x65.

Regarding standard API 5L for pipelines, the maximum component amount allowed for x65 pipeline steel grades are shown following (*Table 1.1*):

Maximum Chemical % of Weight in X65 Steel Grade welded					
C _{MAX}	Mn		P		S _{MAX}
	Min	Max	Min	Max	
0.30	----	1.8	0.045	0.08	0.03

Tab. 1.1 – Maximum Chemical %Weight for x65 (API 5L)

This standard also fix the minimum YS in (*PSI*) that corresponds to the number used to define the steel grade, in this case 65PSI (*448MPa*).

Behavior Study of Pipes after Forming, Coating and Bending

Before 1960s, without API standards, the main materials used were carbon-ferrous based materials instead of alloyed steels ^[5], with typical chemical compositions such appears in *Table 1.2*:

Pipeline Grade	Maximum Weight composition %													
	C	Mn	Si	Al (x10 ²)	Ca (x10 ³)	Ni	N (x10 ²)	Cu	V (x10 ²)	Nb (x10 ²)	Ti (x10 ²)	B (x10 ³)	P (x10 ²)	S (x10 ²)
Basic API 5L	0.31	1.80											3	0.3
API 5L	0.16	1.56	0.35	4			1.2		7	5		1	3	15
Sweet Onshore	0.11	1.56	0.35	4		0.2	1	0.25	8	5			2.5	10
Sweet Offshore	0.08	1.56	0.30	4	3	0.2	0.8	0.25	8	4			1.5	5

Tab. 1.2 – Typical Composition of Pipeline Steels used in 1960s (Source API)

Nowadays, lots of efforts have been done to improve the mechanical properties of pipelines steel grades. Steel strength can be increased by the use of one or a combination of the following mechanisms:

- Solid solution strengthening by addition of alloying elements: C, Si, Mn, etc.
- Grain refining.
- Precipitation strengthening by Microalloying with Nb, Ti, Al, Ni.
- Transformation strengthening by formation of martensite and bainite.
- Dislocation strengthening by work hardening.

Taking into account these mechanisms, during last decades, improved properties have been reached upgrading the steels chemical compositions according manufacturing procedures and in service conditions, and are shown following in *Table 1.3*:

Pipeline Grade	Thickness (mm)	Maximum Weight composition %													
		C	Mn	Si	Al (x10 ²)	Ca (x10 ³)	Ni	N (x10 ²)	Cu	V (x10 ²)	Nb (x10 ²)	Ti (x10 ²)	B (x10 ³)	P (x10 ²)	S (x10 ²)
X65	16	0.02	1.59	0.14			0.17				4	1.7	1	1.8	3
X65	25	0.03	1.61	0.16			0.25				5	1.6	1	1.6	3
X70	20	0.03	1.66	0.14					7	4	1.8		2.5	4	
X70	20	0.06	1.60						0.04		5				

Tab. 1.3 – Typical Composition of Actual Pipeline Steels (Source API^[6])

The chemical compositional changes from 60s until now are due to the role of each element in the material properties, the most important are:

- C – Increases strength (yield and ultimate) and also hardness, but reduces ductility (elongation and rupture) and notch toughness (using high amounts, Charpy tests exhibits nil brittle-ductile transition temperature, BDTT). It also affects weldability, being more difficult to control in the process.
- Mn – Deoxidizes and desulfurizes steel avoiding brittle iron-sulfides, refining the grain and improving hot-workability. It is demonstrated that if ratio $Mn/C > 3$ the Mn improves impact toughness and above 0.8% Mn tends to harden steel.
- Si – Improves castability because of is a deoxidizer that captures dissolved oxygen avoiding porosities.
- Ni – Causes a significant improvement in fracture toughness and fatigue resistance.
- Cu – Improve atmospheric corrosion resistance.
- V – Refines steel grains, improving its mechanical properties and its resistance to H attack.
- S – Is contained in the steel and is considered as an impurity that forms brittle crack-prone iron sulfide.
- P – Increases ultimate strength (US) of the steel. Otherwise is considered an impurity because forms brittle, crack-prone iron-phospite during heat-treatments or at high temperature services.

1.5 PIPELINES COATINGS

Pipelines need to be protected under corrosion effects ^{[1][7]}(CD DOCUMENTATION/COATINGS). The main purpose of coating is to isolate the pipe steel from the environment: soil, seawater, rain, etc. and to present a high resistance path between anodic and cathodic areas. *Table 1.4*, summarizes the different steps with its range of temperatures to apply on coatings processes:

	NAME	PIPE TEMPERATURE (°C)	TIME (s)	OBSERVATIONS
SURFACE	Water washing	Hot water or steam	--	--
	Dry and Preheating	In function of subsequently coating	--	--
	Blast cleaning	--	--	Can affect to mechanical properties
	Coating adhesion	120	At least 20	Chemical pretreatment (phosphoric acid) and chromate conversion coating
COATING	Asphalt Enamel	250 ^{*1} (maximum) Inner preheat at 40°C	--	After coating, quenched. Ts= 65-75°C
	FBE ^[8]	220	--	Electrostatically heated; Ts=70°C
	PE/PU/PP	220	--	Electrostatically heated and water quenched at 80°C. PE Ts=85°C; PU Ts=100°C; PP Ts=75-140°C
	Elastomeric Coating (Neoprene)	145	2 (hours)	P=500 KPa (vulcanization)
	Thermal Insulation	220	--	Electrostatically heated

T_s : Temperature in service; P : Pressure;
*NOTE: Pipe temperature is the temperature of the pipe when the coating is applied. *1 is the maximum reachable temperature of the coating product and not the steel temperature.*

Tab. 1.4 – Pipe surface preparation and coatings summary

As can be observed in *Table 1.4* a previous surface treatment is required for the assurance a good steel surface and to avoid defects on the coating process. Dry and pre-heat stage, is function of the subsequent coating process.

Blast cleaning can affect the mechanical properties of the steel being similar than a micro shoot-penning process, indeed, higher pre-strain value can be induced, *Figure 1.11* , although the heat applied during the coating steps can help to recover partially its initial values.

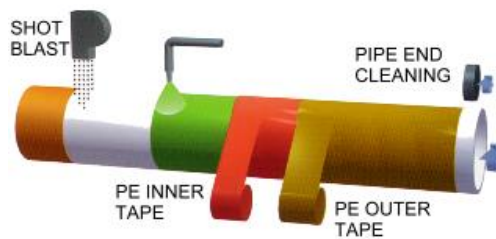


Fig. 1.11– Blast cleaning process

The maximum temperature reached by the pipe steel is 220°C by electrostatically heating. In the case of Asphalt Enamel maximum temperature of 250°C can be reached by the coating product directly applied to the pipe steel.

2 JUSTIFICATION AND OBJECTIVES

Arcelor Mittal delivers hot rolled products from coil for the energy market, which are subsequently formed and welded to produce pipelines for oil and gas transportation. The guaranteed mechanical properties such as yield stress, tensile strength, toughness, elongation, tend to decrease due the forming procedures from coil to pipe. These mechanical properties can be predicted using numerical models capable of describing its evolution during pipe manufacturing. Nonetheless, this guarantee cannot take into account the evolution of the pipe properties during downstream processing. Indeed, once the pipe is sold, it needs to be coated, installed, welded and sometimes bent.

The objective of the project is obtain a better understanding of the influence of the coating, which is a thermal cycle, straining and in field-bending in the mechanical properties of the material.

For this purpose, a study of coating methods has been done, in order to define the industrial pipe thermal cycles. Experimental tests are also carried out to provide a better understanding of the influence of the thermal cycles on the base material once is prestrained due the UOE pipe forming process.

Experimental tests consist on tensile test, to obtain the mechanical properties in both conditions: as received material, it means without coating, and once the material is coated. Energetic test, Charpy V-Notch (CVN) impact test is also necessary for a better understanding of the capability of the material to absorb impact energy and for the determination of the Brittle-Ductile Transition Temperature (BDTT) of the coated material.

CVN impact tests are usually done in a very low range of temperatures. Due that the samples are handled from the freezer to the test machine until hammer impacts on it, only the initial temperature is well known. To know the final CVN sample temperature once the hammer impact an analytical heat transfer model have been developed and validated to predict the temperature. It also means the increase in order to assure the experimental quality on this test.

A Finite Element Model (FEM) simulation is carried out to simulate a general cold bending process to predict the final mechanical properties of x65 steel grade under a cold bending process.

3 EXPERIMENTAL METHODOLOGY

3.1 SAMPLING AND COATING RECREATION

To perform the tests all the samples have been heat treated to recreate using a conventional industrial furnace similar heat conditions that are applied in a real coating industrial pipes processes.

The specimens are taken out in transversal direction, opposite side of the weld, being a base not welded material (*Figure 3.12*), and finally machined by milling.

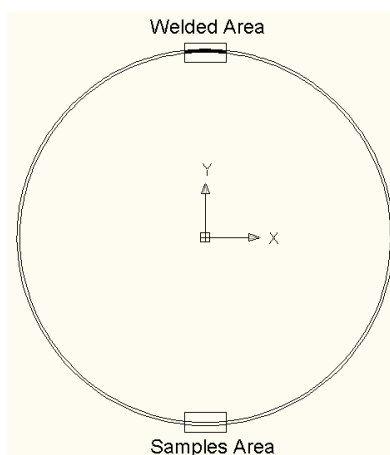


Fig. 3.12 – Samples area base material location

According coating processes, two different temperatures (*minimum and maximum*) and two different times of application (*quickly and slower coating process*) have been selected, as can be seen in the following *Table 3.1*:

Heat treatment ID	Time [s]	Temperature [°C]
T1	30 ^{±2}	140 ^{±1}
T2	300 ^{±2}	140 ^{±1}
T3	30 ^{±2}	245 ^{±1}
T4	300 ^{±2}	245 ^{±1}

Table 3.1: Sample identification

The samples have been introduced inside the industrial furnace, and heated up to selected temperature. At the same time a dummy sample of X65 according standard ISO148-1 for the Charpy sample dimension equipped with a type K thermocouple have been connected to a computer to control the real temperature of the samples and register it. Notice that the tensile samples, have been treated together with the Charpy samples.

3.2 TENSILE TEST

The experimental tests that can be applied to the materials to know their properties can be ^[9]:

- Physical Tests. Hardness, Stress, Impact toughness, Fatigue, Heat transfer, etc.
- Chemical Tests. To know qualitative and quantitative composition, corrosion, etc.
- Physical-Chemical Tests. Macro and microscopically tests with chemical attacks and subsequently physical tests, etc.
- Electrical Tests. Magnetism behaviour, Dielectric breakdown voltage, etc.

Also experimental tests can be categorized in: Destructive or Non- Destructive Tests.

The tensile test is a destructive physical test and is typical used to determine the basic physical properties of the materials that constitute the basic principles of deformation and fracture.

In general, tensile tests are performed on cylindrical specimens (*see Figure 3.16*) or parallel-piped specimens (*sheet and plate*). The samples are loaded uniaxially along the length of the specimen being the applied load and extension (*change in length*) of the sample simultaneously measured ^[10].

The recorded strain and stress depict a typical curve such is following (*Figure 3.13*):

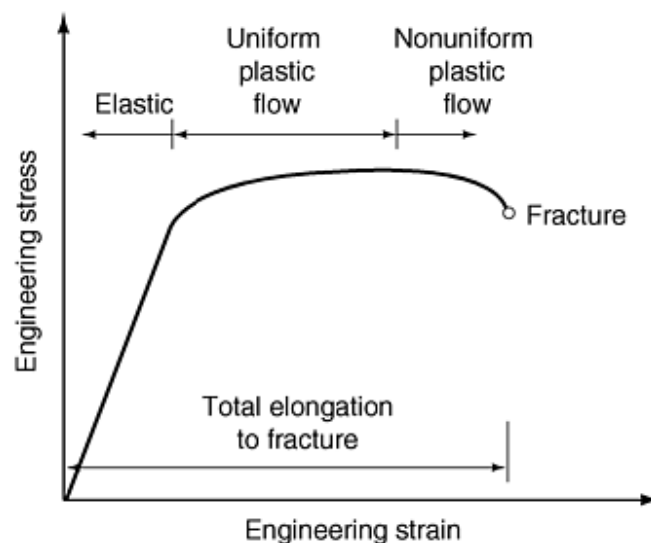


Fig. 3.13 – Typical Engineering Strain-Stress curve

In the elastic and uniform plastic flow areas, the deformation in the sample is homogeneously in the whole cross section despite in Non Uniform plastic flow Area the deformation appears focused in the central section of the sample due the material striction exhibiting the classical neck form (*according to Schmidt's Law*), where the sample broke.

3.2.1 MECHANICAL PROPERTIES

The main mechanical properties to obtain from tensile test are:

3.2.1.1 ENGINEERING STRESS AND ENGINEERING STRAIN

Engineering stress (σ_n) is defined like the quotient between the applied uniaxial force and the initial sample cross section:

$$\sigma_n = \frac{P}{A_o}$$

(Eq. 1)

Where:

- P : Applied force [N]
- A_o : Initial Sample Cross Section [m²]
- $[\sigma_n] = \left[\frac{N}{m^2} \right] = \left[\frac{Kp}{mm^2} \right] = [Pa]$

Engineering strain (ε_n) is defined like the quotient between length increment (*change of length*) and the initial length:

$$\varepsilon_n = \frac{\Delta l}{l_o} = \frac{l_f - l_o}{l_o}$$

(Eq. 2)

Where:

- l_o : Initial length of the sample
- l_f : Final length of the sample

This analysis facilitates the comparison of results obtained when testing samples that differ in thickness or geometry.

3.2.1.2 TRUE STRESS AND TRUE STRAIN

Although engineering values are adequate, the best measures of the response of a material to loading are the true stress (σ) and true strain (ε) determined, in this case, by the instantaneous dimensions of the tensile specimen due to the changes while the force is applied. It consists in the increase of the length in the axial direction with a parallel decrease, however and in the same time, in the cross section.

Because the instantaneous dimensions of the specimen are not typically measured, the true stress and true strain may be estimated using the engineering stress and engineering strain. It is noted that these estimations are only valid during uniform elongation and are not applicable throughout the entire deformation range.

True strain is defined like the quotient between the changes in the length and the instant length:

$$d\varepsilon_r = \frac{dl}{l}$$

So:

$$\varepsilon_r = \ln\left(\frac{l_f}{l_o}\right) = \ln(\varepsilon_n + 1)$$

(Eq. 3)

And assuming that the sample has not any change in its volume, using *equation 3*, true stress can be defined as follows:

$$\sigma_r = \sigma_n(\varepsilon_n + 1)$$

(Eq. 4)

3.2.1.3 TENSILE STRENGTH

The tensile strength is a term which refers to the amount of tensile stress that a material can withstand just before the effective fracture or failure. It is equivalent to the maximum load (P_{MAX}) that can be carried by one square millimeter of cross-sectional area when the load is applied as uniaxial stress, and can be defined using the following expression:

$$\sigma_{TS} = \frac{P_{MAX}}{A_o}$$

(Eq. 5)

3.2.1.4 YIELD STRENGTH

In the initial stages of deformation, generally stress changes linearly with the strain. In this region, all deformation is considered to be elastic because the sample will return to its original shape (*initial dimensions*) when the applied stress is removed. If, however, the sample is not unloaded and deformation continues, the stress-versus strain curve becomes nonlinear causing a permanent elongation named plasticity.

The stress at which a permanent deformation occurs is called the elastic (*or proportional*) limit; however, offset yield strength (*0.2% and 0.5% of offset*) are typically used to quantify the onset of plastic deformation due to the ease and standardization of measurement.

3.2.1.5 DUCTILITY

Ductility is the ability of a material to deform plastically without fracturing. The test sample elongates during the tension test and correspondingly reduces its cross-sectional area. These two measures of the ductility of a material are the amount of elongation and reduction in area that occurs during the tension test and can be expressed like the following equation:

$$A_{PROP}(\%) = \frac{l_f - l_o}{l_o} \times 100$$

(Eq. 6)

3.2.1.6 STRAIN-HARDENING EXPONENT

The flow curve of many metals in the region of uniform plastic deformation can be expressed by the following simple power curve expression:

$$\sigma = K\varepsilon^n$$

(Eq. 7)

Where:

- n : Strain-hardening exponent
- K: Strength coefficient to reach $\varepsilon=1$.

3.2.1.7 RESILIENCE ^[11]

Resilience is the property of a material to absorb energy when it is deformed elastically recovering it once unloading. In other words, it is the maximum energy per unit volume elastically stored. It is represented by the area under the curve in the elastic region in the Stress-Strain diagram (Figure 3.14) and can be expressed as follows:

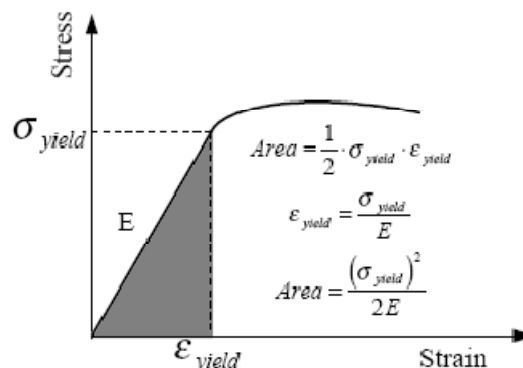


Fig. 3.14 – Typical Engineering Strain-Stress curve

3.2.1.8 TOUGHNESS

The toughness of a material is its ability to absorb energy in the plastic range ^[12]. Toughness may be considered to be the total area under the stress-strain curve (*Figure 3.15*) which is referred to as the modulus of toughness (*UT*) is an indication of the amount of work per unit volume that can be done on the material without causing it to rupture.

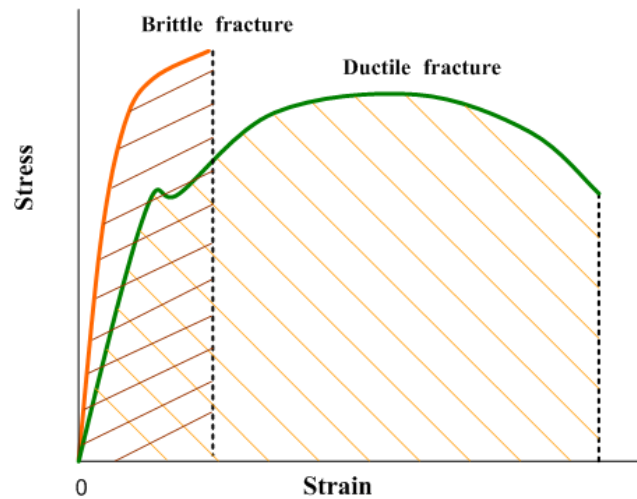


Fig. 3.15 – Typical Engineering Strain-Stress curve

As can be observed in the *Figure 3.15* two different main groups of toughness are showed referenced with the most important types of fractures (*see Chapter 3.4.2*), brittle and ductile fracture. The ductile fracture (*green curve*) corresponds with the higher area indicating that more amount of energy can be absorbed for the material before fracture. It is due the high plasticity of the material.

The orange curve corresponds with the opposite case, the brittle fracture with quite less area showing clearly that lower plasticity is supported.

The ability to withstand occasional stresses above the yield stress without fracturing is particularly desirable in pipelines (*ductile fracture behavior*).

3.2.2 EXPERIMENTAL TENSILE TEST DESCRIPTION

All tensile tests are performed on an electro-mechanical testing machine Zwick Z250.

During the tensile test 2 crosshead speeds are used, namely:

- First traverse speed: position controlled 20MPa/s from: start until Rp0.2.
- Second traverse speed: position controlled 0.00025/s from Rp0.2 until fracture.

Each tensile test is made for each heat treatment and for it, 3 different specimens have been tested, identifying (*ID*) each specimen.

The sample description is given in Table 3.2:

Sample ID	Description	Material
Base-x	Base material	Material x65 Pipe #3 After PWHT Diameter 24", Wall thickness 14.8 mm Pipe ID H473/6-52 5/11 Coil 1737040
T1-x	Simulation 1	
T2-x	Simulation 2	
T3-x	Simulation 3	
T4-x	Simulation 4	

x: repetition 1 to 3

Table 3.2: Sample identification

The tensile tests are performed on round API specimens (*Figure 3.16*), according to standard ASTM A370, with a nominal diameter of $6.300^{±0.005}$ mm, $L_c = 30.000^{±0.010}$ mm and reference length $L_o = 25.000^{±0.050}$ mm.

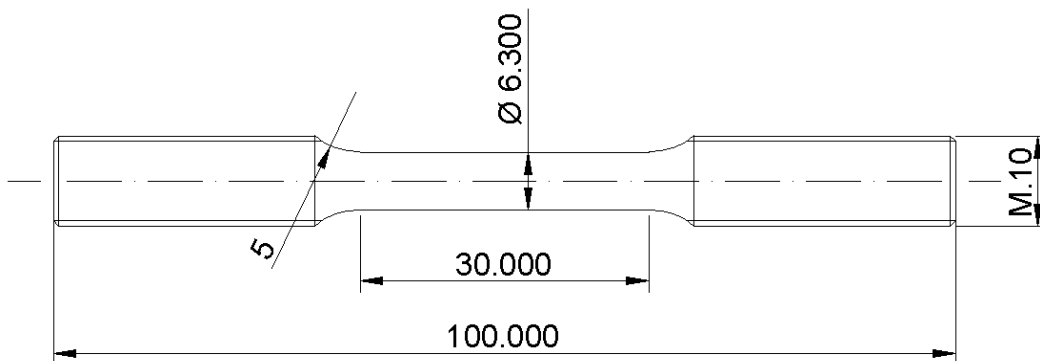


Fig. 3.16 – Tensile test ASTM A370 sample

3.3 HEAT TRANSFERS IN CHARPY V-NOTCH

Charpy Impact tests are very common and usefully to obtain information of the materials subjected to dynamic loads ^{[13][14]} (see Chapter 3.4) being very interesting to know the value of the temperature in the sample during the whole test. To solve this issue, is necessary previous basic knowledge of thermodynamics.

Two bodies at different temperature tend to compensate it, until the same temperature is reached for both^[15]. This is accomplished by the transfer of energy from the warm medium to the cold one so the energy transfer is always from the higher temperature medium to the lower temperature one. The temperature difference is the driving force for heat transfer.

The rate of heat transfer in a direction depends on the magnitude of the temperature gradient (*the temperature difference per unit length, ΔT*) in that direction. The larger ΔT , the higher the rate of heat transfer.

Energy can exist in numerous forms, such as thermal, kinetic, potential, etc. and their sum constitutes the total energy (E) of a system. The forms of energy related to the molecular structure of a system and the degree of the molecular activity are referred to as the microscopic energy. The sum of all microscopic forms of energy is called the internal energy of a system, U [J].

The internal energy may be viewed as the sum of the kinetic and potential energies of the molecules. The average velocity and the degree of activity of the molecules are proportional to the temperature. Thus, at higher temperatures the molecules will possess higher kinetic energy, and as a result, the system will have a higher internal energy. This internal energy is also associated with the intermolecular forces between the molecules of a system, forces that bind the molecules to each other in each matter.

3.3.1 ENERGY TRANSFER

Heat transfer between matters implies energy transferring. This energy can be transferred from a given mass by two mechanisms: heat (Q) and work (W).

In case of a closed system, without mass exchange, first law of thermodynamics of the conservation of energy defines that the states that energy can neither be created nor destroyed; it can only change forms:

$$\left(\begin{array}{c} \text{Total Energy} \\ \text{entering the} \\ \text{system} \end{array} \right) - \left(\begin{array}{c} \text{Total Energy} \\ \text{leaving the} \\ \text{system} \end{array} \right) = \left(\begin{array}{c} \text{Change in the} \\ \text{total energy of} \\ \text{the system} \end{array} \right)$$

And can be defined as the follow equation:

$$\frac{dU}{dt} = Q - W$$

(Eq. 8)

In the absence of significant electric, magnetic, motion, gravity, and surface tension effects, $W=0$, the change in the total energy of a system during a process is simply the change in its internal energy (U).

$$E_{in} - E_{out} = \Delta U = mC_p\Delta T = Q [J]$$

(Eq. 9)

The heat is transferred by the mechanisms of conduction, convection and radiation (Figure 3.17) [16]:

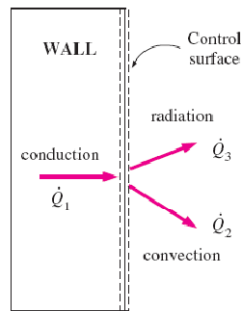


Fig. 3.17 – Heat transference mechanisms

And the total amount of Q in the global system can be expressed as:

$$Q = Q_{COND} + Q_{CONV} + Q_{EMIT,MAX}$$

(Eq. 10)

• CONDUCTION

Is the transfer of energy from the more energetic particles of a substance to the adjacent less energetic ones as a result of interactions between the particles. In solids, heat conduction is due two effects: the lattice vibrational waves induced by the vibrational motions of the molecules positioned at relatively fixed positions in a periodic manner called a lattice, and the energy transported via the free flow of electrons in the solid.

The rate of heat conduction through a medium depends on the geometry of the medium, its thickness, and the material of the medium, as well as the temperature difference across the medium.

Fourier's law defines the heat conduction as follows:

$$Q_{cond} = -kA \frac{dT}{dx} [W]$$

(Eq. 11)

Where:

- k : thermal conductivity of the material, which is a measure of the ability of a material to conduct heat (*constant with dependence of the temperature*).
- dT/dx : the temperature gradient.
- A : heat transfer area - always normal to the direction of heat transfer [m^2].

- **CONVECTION**

Is the mode of energy transfer between a solid surface and the adjacent liquid or gas that is in motion, and it involves the combined effects of conduction and fluid motion. The faster the fluid motion, the greater the convection heats transfer.

Two possible cases of convection are possible depending on the fluid motion:

- Natural convection - when the fluid motion is caused by buoyancy forces that are induced by density differences due to the variation of temperature in the fluid
- Forced convection – when the fluid is forced to flow over the surface by external means such as a fan, pump, or the wind.

Newton's law defines the heat convection as follows:

$$Q_{conv} = hA(T_s - T_{\infty}) [W] \quad (Eq. 12)$$

Where:

- h : the convection heat transfer coefficient [$W/m^2 \text{ } ^\circ C$].
- A : the surface area through which convection heat transfer takes place [m^2].
- T_s : the surface temperature [K].
- T_{∞} : the temperature of the fluid sufficiently far from the surface [K].

- **RADIATION**

Is the energy emitted by matter in the form of electromagnetic waves as a result of the changes in the electronic configurations of the atoms. Unlike conduction and convection, the transfer of energy by radiation does not require the presence of an intervening medium.

Heat transfer studies are focused in thermal radiation, which is the form of radiation emitted by bodies because of their temperature.

Stefan-Boltzmann law defines the heat radiation as follows:

$$Q_{emit,max} = \sigma A_s T_s^4 [W] \quad (Eq. 13)$$

Where:

- $\sigma = 5.67 \cdot 10^{-8} [W/m^2 \cdot K^4]$ (Stefan-Boltzmann constant)
- T_s : Absolute temperature of the surface [K]
- A_s : Surface area [m^2]

Radiation is usually significant relative to conduction or natural convection, but negligible relative to forced convection. Thus radiation in forced convection applications are usually disregarded, especially when the surfaces involved have low emissivities and also from low to moderated temperatures.

3.3.2 ANALYTICAL DESCRIPTION

Following, an analytical description to solve the heat transfer is described. Previously, is needed to ensure which are the mechanisms present in each phase of the test.

Knowing that heat transfer involves the mechanisms of conduction, convection and radiation and focusing on the *equation 8* the $W=0$ and $Q=Q_{COND}+Q_{CONV}+Q_{EMIT,MAX}$, then can be assumed that:

3.3.2.1 CONDUCTION MECHANISM

In the first phase of the test the sample is taking out of the fridge, and do not have physical contact with any solid conductible surface (see *Figure 3.20 in following Chapter 3.3.3*). It means that:

$$Q_{COND}=0W$$

3.3.2.2 RADIATION MECHANISM

According to Stefan-Boltzmann law for radiation definition, at an initial temperature of $-150^{\circ}C$ ($123K$), the heat transmitted by the system can be calculated as follows:

$$Q_{emit,max} = \sigma A_s T_s^4$$

$$Q_{emit,max} = 5.67 * 10^{-8} * 2.20 * 10^{-3} * 123^4 = 0.028W$$

As can be seen above, the term temperature (T) is more important as the temperature increase, so considering a maximum significant value of the temperature of $-50^{\circ}C$ ($223K$) the heat transmitted reaches a value of:

$$Q_{emit,max} = 0.308W$$

Following the approximate value of Q_{conv} is calculated for natural and forced convection:

$$Q_{conv,natural (123K)} = 9W ; Q_{conv,forced (123K)} = 134W$$

$$Q_{conv,natural (223K)} = 2W ; Q_{conv,forced (223K)} = 13W$$

As it is known, natural convection is the case with less heat transfer, and as can be seen, the value of heat transfer is much higher than the obtained value for radiation heat transfer, representing a maximum discrepancy of 15%.

It means that heat transfer by radiation will be neglected because the DBTT in the Charpy tests for X65 is often lower than $-30^{\circ}C$ due the difference in the Q for radiation versus convection cases.

3.3.2.3 CONVECTION MECHANISM

Has been determined that only convection mechanism is the main driver force for the heat transfer in CVN Impact Test. Following the procedure to predict the final sample temperature in function of time by convection, is described:

Considering the next hypothesis when $W=0$, *equation 8* can be rewritten as:

$$\frac{dU}{dt} = Q$$

And the energetic balance equilibrium as:

$$E_{in} - E_{out} = \Delta U$$

Neglecting the contribution of the radiation:

$$Q_{total} = Q_{cond} + Q_{conv}$$

Then the losses of heat in the sample have to be the same than the fluid wins:

$$\Delta Q_{sample} = -\Delta Q_{air}$$

Meaning that the heat that loses the sample by conductivity is the same that the heat won by the air by convection:

(Heat transfer into the body during dt = Increase in the energy of the body during dt)

$$Q_{cond} = Q_{conv}$$

Knowing that a constant pressure, the amount of energy transferred to air is the change in its enthalpy (ΔH):

$$\Delta H = mC_p\Delta T$$

(Eq. 14)

Where:

- m : mass of the body [Kg].
- C_p : Specific heat of the body [J/KgK].
- ΔT : Increment of temperature ($T_{initial} - T_{\infty (room)}$).

And assuming that:

- $T_{\infty} > T_i$.
- $dt = d(T-T_{\infty})$ and T_{∞} =constant value.

The expression $Q_{\text{cond}} = Q_{\text{conv}}$ can be written as:

$$A_s h (T_{\infty} - T) dt = m C_p dT$$

(Eq. 15)

Grouping terms and isolating the variables:

$$\frac{A_s h}{m C_p} dt = \frac{dT}{T_{\infty} - T}$$

Then knowing that $m = \rho V$:

Where:

- ρ : density [Kg/m³].
- V : volume [m³].

$$\frac{-A_s h}{\rho V C_p} dt = \frac{d(T - T_{\infty})}{T - T_{\infty}}$$

And taking the limits for the integration as: $t_0 \rightarrow t$ and $T_i \rightarrow T=T(t)$ and grouping the constants:

$$B = \frac{-A_s h}{\rho V C_p}$$

(Eq. 16)

It can be simplified as:

$$B \int_{t_0}^{t_f} dt = \int_{T_i}^{T_f(t)} \frac{d(T - T_{\infty})}{T - T_{\infty}}$$

Obtaining:

$$Bt = \ln \frac{T(t) - T_{\infty}}{T_i - T_{\infty}}$$

And finally obtaining heat transfer general equation:

$$e^{-Bt} = \frac{T(t) - T_{\infty}}{T_i - T_{\infty}}$$

(Eq. 17)

Once it is know the procedure to calculate the heat transfer in convection, it is strongly dependent of the type of convection in the system that can be natural or forced convection.

3.3.2.3.1 NATURAL CONVECTION

Natural convection appears when the fluid motion occurs by natural means such as buoyancy involving, usually, very low fluid velocities. The buoyancy force is caused by the density difference between the heated or cooled fluid adjacent to the surface and the fluid surrounding it, and is proportional to this density difference and the volume occupied by the warmer fluid. The gravitational acceleration causes the fluid movement because of the density difference.

The flow regime in natural convection is governed by the dimensionless Grashof number, which represents the ratio of the buoyancy force to the viscous force acting on the fluid.

This number provides also the main criterion in determining whether the fluid flow is laminar or turbulent in natural convection because of the h constant dependence. The Grashof number can be calculated as:

$$Gr = \frac{g\beta\Delta T X^3}{\nu^2}$$

(Eq. 18)

Where:

- g : Gravitational acceleration [m/s^2].
- β : Coefficient of volumetric thermal expansion [$1/K$].
- ΔT : Increment of temperature [K].
- X : Characteristic length of the geometry [m].
- ν : Kinematic viscosity of the fluid [$Kg/m\ s$].

Assuming that:

- $\beta = 1/T$ for ideal gases, will be assumed that in air environment, $\beta=1/T_f$ being $T_f=T_\infty$.
- X : the characteristic length for the rectangular sample case, will be $L_c = \frac{A_s}{p} = \frac{L^2}{4L} = \frac{L}{4}$.
- ν : the kinematic viscosity of the air at $\overline{T_f = \frac{|T_l + T_\infty|}{2}}$, will be considered in function of the changes in the increment of the temperature between the sample and the room.

Once the Grashof number is determined, according experimental standard values for these geometrical conditions is needed to know which the flow regime is, it means laminar or turbulent flow.

For this purpose, it is necessary to calculate the Rayleigh number (Ra):

$$Ra = Gr * Pr$$

(Eq. 19)

Where:

- Gr : Grashof dimensionless number.
- Pr : Prandtl dimensionless number, which takes into account the relation between heat transfer and the quantity of movement transfer.

And if:

$$Ra < 10^9 \rightarrow \text{Laminar flow}$$

$$Ra > 10^9 \rightarrow \text{Turbulent flow}$$

Then, knowing the type of flow, Nusselts (Nu) number can be calculated as:

$$Nu = \frac{hL_c}{k} = C(GrPr)^n K = CRa^n K$$

(Eq. 20)

Where:

- k : Fluid thermal conductivity [W/m°C].
- C and n : constants dependent of the geometry of the surface and flow regime:
 - N=1/4 : Laminar flow
 - N=1/3 : Turbulent flow
- K : Dimensionless correction function.

Finally the value of the h can be calculated to know the B value in the main heat transfer equation described above (Equation 16):

$$h = \frac{Nuk}{L_c}$$

(Eq. 21)

3.3.2.3.2 FORCED CONVECTION

In forced convection, is quite noticeable, since a fan or a pump can transfer enough momentum to the fluid to move it in a certain direction.

The convection heat transfer coefficient is strongly dependent of the velocity: the higher the velocity, the higher the convection heat transfer coefficient, being much higher in forced convection than in natural convection. In this case, as in natural convection, difference in the densities is present, but affected primarily by the forced velocity at which is obligated to flow the fluid.

As it expect, the h values for forced convection will be higher for forced convection than for natural convection.

Same considerations than natural convection have to be taken into account, however, some other parameters needs to be added.

For these cases, according to the geometrical conditions, rectangular cross section, and the standards definitions, Re can be calculated as:

$$Re = \frac{VX}{\nu'}$$

(Eq. 22)

Where:

- V: Velocity of the fluid [m/s].
- X: Characteristic length of the geometry [m].
- ν' : Dynamic viscosity of the fluid [m²/s].

Knowing the Re constant value, the standards defines the following equation to calculate Nu for cylinders of others cross sections different than circular cylinders:

$$Nu = 0.43 + CRe^m$$

(Eq. 23)

Where:

- C and m: Dimensionless constant

And finally the h value can be obtained using the *equation 21*.

3.3.3 EXPERIMENTAL HEAT TRANSFER CHARPY V-NOTCH PROCEDURE

The experimental procedure for this test, have been manage recreating the same conditions needed to conduct a Charpy V-Notch test according to the standard ISO 148-1: Charpy pendulum impact test "Part1: Test method".

The Charpy samples (Figure 3.18) have been made according standard ISO 148-1:

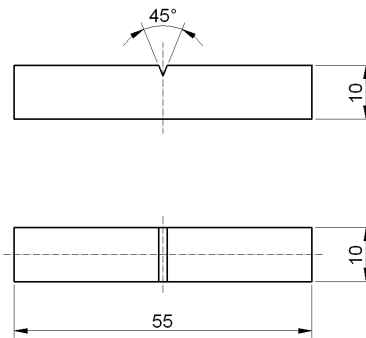


Fig. 3.18 – Charpy V-Notch ISO 148-1 Samples dimensions

The tests are conducted at different temperatures (between $-100\text{ }^{\circ}\text{C}$ and $0\text{ }^{\circ}\text{C}$ using $20\text{ }^{\circ}\text{C}$ of each increment). For lower temperatures (up to $50\text{ }^{\circ}\text{C}$ or higher) than the room temperature samples are cooled using chilled Thermo Electron Cryomed Freezer nitrogen refrigerator. From the moment the dummy sample (equipped with thermocouple Type K) has reached the desired temperature is maintained that at least 30 minutes before proceeding to testing (Figure 3.19).

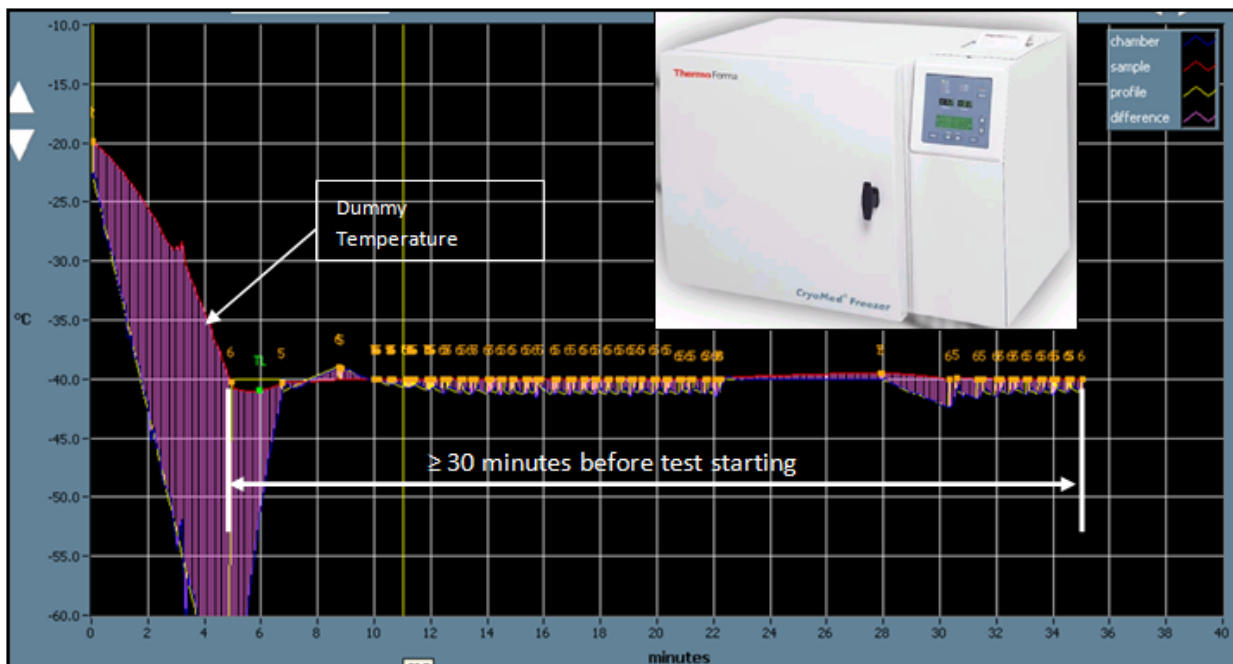


Fig. 3.19 – Thermo Electron Cryomed freezer

The dummy with thermocouple type K (Figure 3.18) is connected to a computer, and using Picolog Recorder software, the temperature of the sample is registered in each time instant. The time step for each data recording defined is 10ms.

The registered time has been until 9 seconds, due that the maximum time needed for the sample, until fracture is in the worst case, 7 seconds.

After this time, the sample is handled and positioned in the Charpy Test Machine. According to a previous internal OCAS study ^[17], the samples have been handled using isolated tongs as can be seen below (Figure 3.20):

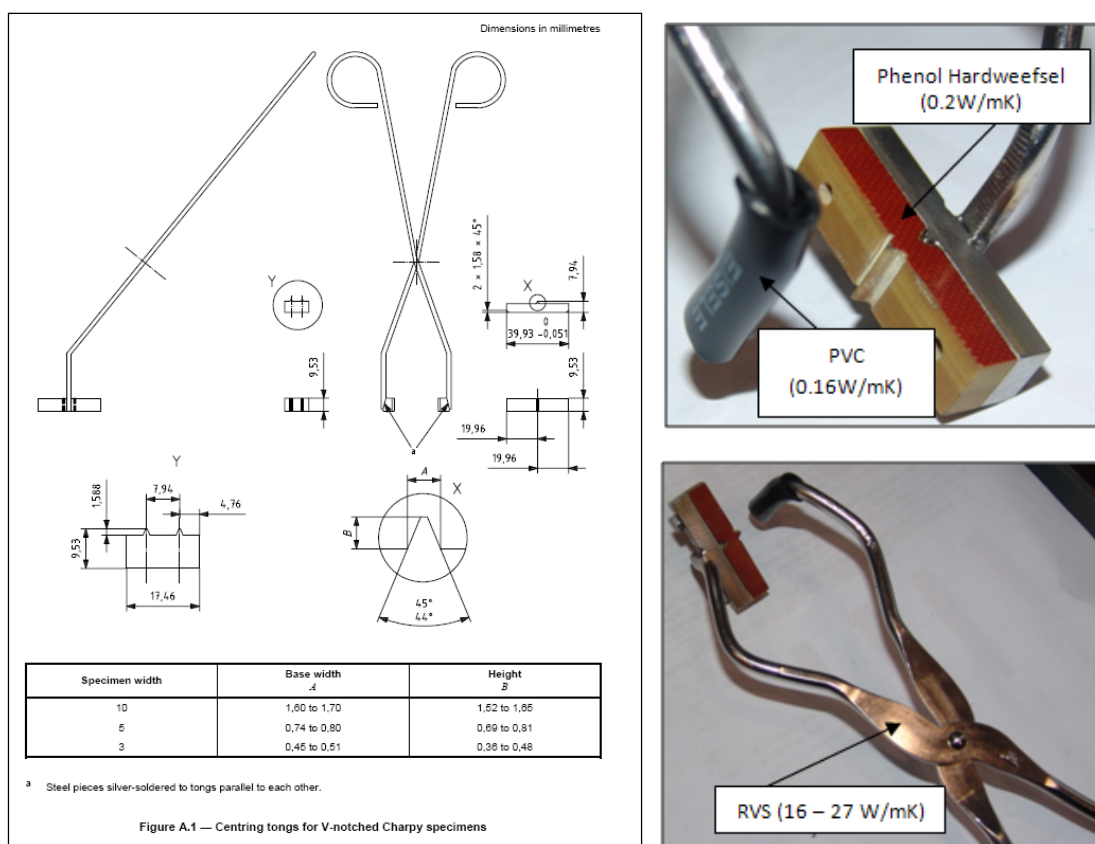


Fig. 3.20 – Isolated tongs specification

The isolated tongs, are cooled at the same temperature than the samples, so it can be concluded that the conductivity can be neglected in the analytical model (as mentioned above in Chapter 3.3.2.1).

3.4 CHARPY V-NOTCH IMPACT TEST

Toughness has been defined as the ability of a material to absorb energy (*see Chapter 3.2.1.8*). Using tensile-strain tests, the toughness can be determined in static or quasi-static conditions due to the load is applied gradually by slow and progressive procedure. Regarding this type of experimental tests, it only reflects also planar stress system, because the uniaxial applied stresses.

Nowadays, it is well known that lots of fractures in materials happens when dynamic loads are applied not predicted only using static load experimental test to know the behaviour of the material.

A proper use of fracture-mechanics methodology for fracture control of structures necessitates the determination of fracture toughness for the material at the temperature and loading rate representative of the intended application.

Charpy tests, is one of the most common test to introduce 3D stress, not only planar stresses, applied in dynamical condition, giving results more closed to the real in service conditions. This application is very useful to determine the non-uniform plasticity behaviour of the material using micro-mechanical mathematical models, to predict elastic-plastic non-linear fracture behaviour of the material taking into account energetic criteria.

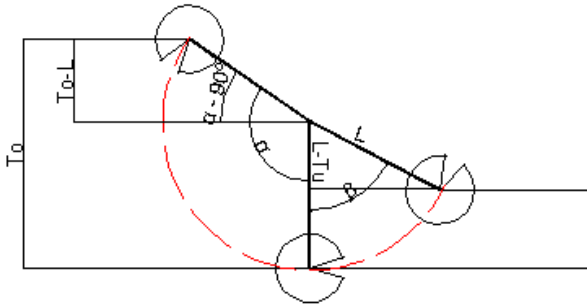
The Charpy V-notch impact specimen is the most widely used specimen for material development, specifications, and quality control.

The values that can be obtained with these tests are not directly easy to use like in tensile tests to know physical constants for engineering calculations; however all of these values provide predictable conclusions once the material is subjected to real conditions: Ductile-Brittle Transition Temperature (*DBTT*), Toughness in dynamic conditions.

This project is focused in the DBTT and toughness of the material and not in elastic-plastic linear and non-linear fractures methods.

3.4.1 CHARPY TEST METHOD

As can be seen in the *Figure 3.23*, the apparatus consists of a pendulum hammer swinging at a notched sample of material. The energy transferred to the material can be inferred by comparing the difference in the height of the hammer before and after a big fracture, as is following described knowing that:



Potential Initial Hammer Energy = $P \cdot h$

Potential Final Hammer Energy = $P \cdot h'$

Potential Consumed Energy = $E_i - E_f = P (h - h')$

Then looking the angles and heights:

$$\sin(\alpha - 90^\circ) = \frac{h - L}{L} ; \sin(\alpha - 90^\circ) = -\cos \alpha ; -\cos \alpha = \frac{h - L}{L}$$

So:

$$L(-\cos \alpha) = h - L ; L + L(-\cos \alpha) = h ; h = L(1 - \cos \alpha)$$

And:

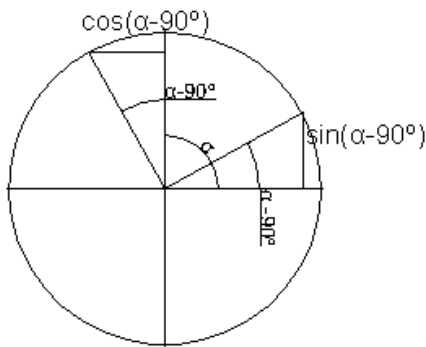
$$\cos \beta = \frac{L - h'}{L} ; h' = L(1 - \cos \beta)$$

Can be obtained that:

$$(h - h') = L(1 - \cos \alpha) - L(1 - \cos \beta) = L(\cos \beta - \cos \alpha)$$

Finally:

$$\varphi = \frac{A}{S} = \frac{PL(\cos \beta - \cos \alpha)}{S} = \left[\frac{Kgm}{cm^2} \right]$$



The results then can be:

- **Quantitative Results**

- The φ is the resilience value directly readed from machine in terms of energy [J] due the heights differences. This is the energy needed to fracture a material and can be used to measure the toughness of the material.
- The DBTT may be derived from the temperature where the energy needed to fracture the material drastically changes. However, in practice there is no sharp transition and so it is difficult to obtain a precise transition temperature. An exact DBTT may be empirically derived in many ways.

- **Qualitative Results**

- The results can be used to determine the ductility of a material. If the material breaks on a flat plane, the fracture was brittle, and if the material breaks with jagged edges or shear lips, then the fracture was ductile. Usually a material does not break in just one way or the other, and thus comparing the jagged to flat surface areas of the fracture will give an estimate of the percentage of ductile and brittle fracture.

3.4.2 MECHANICAL FRACTURES AND DBTT IN CHARPY

Fracture can be defined as the mechanical separation of a solid due to the application of stress. Fractures of engineering materials are broadly categorized as ductile or brittle ^[18].

DUCTILE FRACTURE

This type of fracture is characterized by high strain rates (*high amount of plasticity*) before the fracture. These high strain rates can be localized near the cracks and its propagation is usually very stable, stress need to be increased for the crack propagation.

Ductile fracture is caused by the formation and growth of the voids that eventually comprise the fracture surface. Thus, the toughness of ductile metals is related to the factors that influence the nucleation and growth of voids. Voids nucleate preferably at second-phase particles, such as inclusions and precipitates and as a result of interfacial separation, fracture of the particle or matrix separation is caused by strain concentration near the particle.

Voids grow and coalesce by ductile tearing of the matrix. Ductile tearing resistance is a function of the strength and ductility of the matrix. As matrix strength increases, less energy is dissipated by plastic deformation during tearing, and toughness is reduced. Increased matrix strength also tends to activate additional void nucleation sites. Consequently, yield strength is inversely proportional to fracture toughness

BRITTLE FRACTURE

Brittle fracture requires less energy for surface formation than ductile fracture. Lower energy fracture modes include cleavage and intercrystalline (*grain-boundary*) fracture.

Cleavage is a fracture mode in which material separation proceeds along preferred crystallographic planes without sizable plastic deformation prior to fracture. Metals subject to cleavage usually have a large increase in yield strength as temperature is decreased.

Cleavage occurs when the cleavage fracture stress is reached before the energy required for void formation is exceeded. Intercrystalline fracture occurs when the cohesive strength of the grain boundary is exceeded before cleavage or ductile fracture occurs. As matrix strength increases with decreasing temperature, intergranular failure may occur more readily in a susceptible alloy.

A fracture surface failed in a brittle manner, shows glittering crystalline appearance because of the flat facet produced by failure across the planes in the material.

BDTT

Some materials exhibit brittle fracture behaviour at low temperatures rates. Above a certain limit temperature value this behaviour turns into ductile fracture, increasing ductility values up to high values.

This temperature is well known like Brittle-Ductile Temperature Transition (*BDTT*) and in steels this transition is associated to a change in fracture mechanisms.

The rate of change from ductile to brittle behaviour depends on many parameters, including strength and composition of the material. Because the transition occurs over a range of temperatures, it has been normal to define a single temperature within the transition range that reflects the behaviour of the steel under consideration.

Crystal structure is a reliable guide for qualitative prediction of temperature dependence:

- Face-centered cubic (*FCC*) alloys typically exhibit high toughness throughout the ambient very low range of temperature.
- Body-centered cubic (*BCC*) alloys exhibit precipitous decreases in fracture toughness at critical transition temperatures.
- Hexagonal close-packed (*HCP*) alloys are noted for comparatively low toughness at all temperatures.

Then this transition in BCC and HCP crystal structures becomes at low temperatures, typically below -20°C , when the crystal lattice becomes closer together as the material shrinks. The closer packing of the BCC lattice restricts the degree of shrinkage that is possible. A lower bound is reached beyond which further shrinkage is not possible and as consequence the material has no residual elasticity remaining to absorb the impact energy and fails in a brittle manner by cleavage between the crystal planes.

Typical CVN Fracture Energy Transition is following showed (*Figure 3.21*) with the main 3 test parameters:

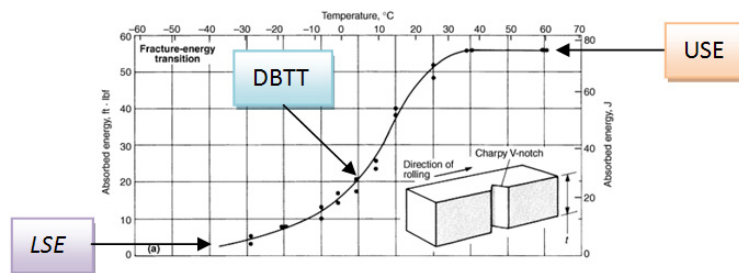


Fig. 3.21 – CVN Fracture Energy Transition Curve

- USE – *Upper Shelf Energy* – Maximum value of the impact energy at entirely ductile material behaviour.
- LSE – *Lower Shelf Energy* – Low level of energy featured with cleavage fracture with low energy demands. Entirely brittle material behaviour.
- DBTT – *Ductile-Brittle Transition Temperature* – Transition zone with mixed material behaviour.

3.4.3 EXPERIMENTAL CHARPY V-NOTCH PROCEDURE

The delivered samples took from X65 base material have been ID as can be seen in Table 3:

Cycle	Samples ID										
Base	3	11	16	21	49	55	60	69	70	87	91
T1	2	5	6	10	12	14	30	31	32	36	40
	45	46	48	57	58	61	71	74	77	79	96
T2	15	23	24	25	27	37	42	56	62	64	65
	73	75	76	80	83	88	89	92	94	95	99
T3	1	8	9	22	26	29	33	34	38	39	41
	44	47	51	52	53	54	63	66	67	97	98
T4	4	7	13	17	18	19	20	28	35	43	50
	59	68	72	78	81	82	84	85	86	90	93

Table 3.3 – Charpy V-Notch Samples Identification

The Charpy samples are sawn and grinded transverse to the pipe into ISO148-1 dimensions (Figure 3.22 & Table 3.4) with subsized dimensions (6.7mm width). The V-notch itself is applied by grinding.

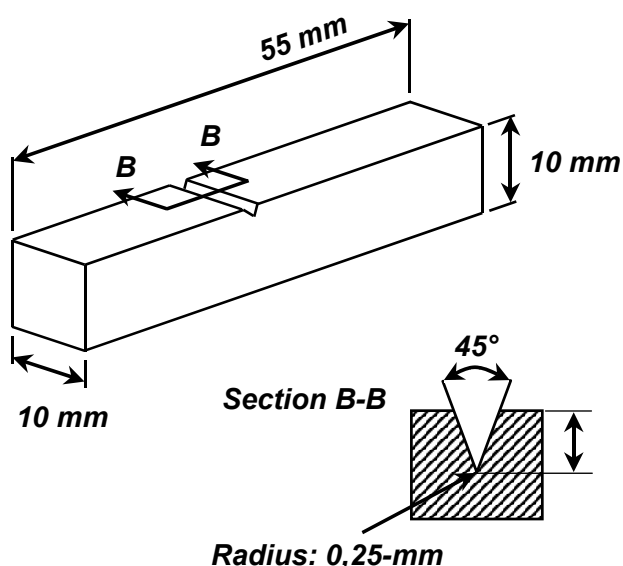


Fig. 3.22 – Charpy sample dimensions

Dimensions	Nominal dimension (mm)	Tolerance (mm)	Minimum dimension (mm)	Maximum dimension (mm)
Length	55.0	±0.6	54.4	55.6
Height	10.000	±0.075	9.925	10.075
Width	10.000	±0.11	9.89	10.11
Notch Angle	45°	±2°	43°	47°
Height below Notch	8	±0.075	7.925	8.075
Radius	0.250	±0.025	0.225	0.275
Notch Position	27.5	±0.42	27.08	27.92

Table 3.4 – Charpy V-Notch Samples Dimensions

As mentioned above the Charpy impact tests are conducted according to the standard according to ISO 148-1: Charpy pendulum impact test "Part1: Test method".

The tests have been done following the same procedure described in *Chapter 3.3.3* also with the same equipment and conditions. The range of temperatures used has been from 0°C until -100°C using increments of -20°C. For each temperature, 3 samples have been tested.

The tests are carried out using 750J Charpy hammer (*Figure 3.23*):

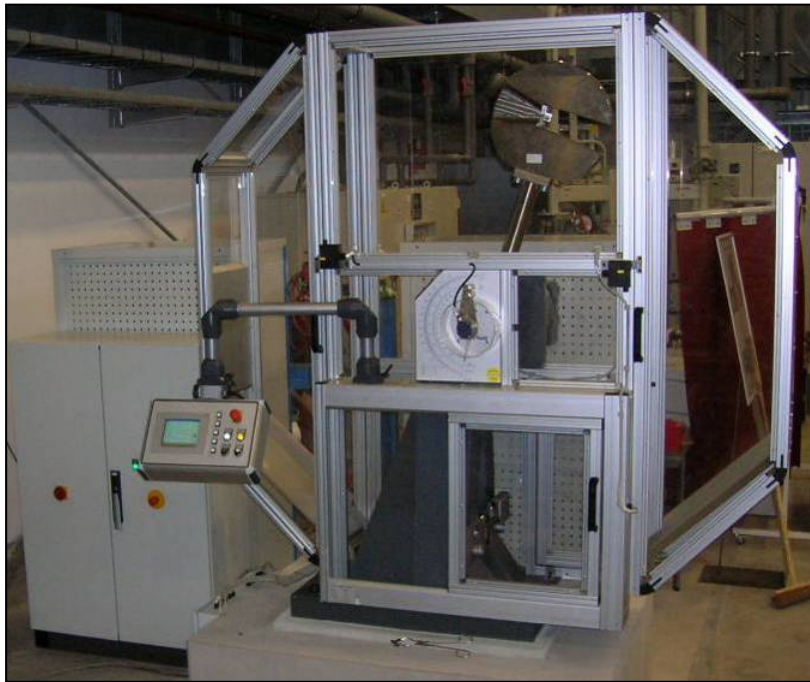


Fig. 3.23 – Charpy test Machine

Once the samples are tested and the results plotted as in *Figure 3.21* an exponential fitting can be done in order to quantify the energy that can be absorbed by the sample in function of the temperature.

3.5 FEM SIMULATION

Nowadays the Finite Elements Methods simulation (*FEM*) has become one of the most important procedures for multi-physical linear and non-linear computational cases of study.

To use any of the actual software existing for these purposes, the main starting point consists assuming the continuum mechanical behavior which consists in a finite number of parts or elements which at the same time, are connected with the surrounding elements by a discrete number of nodes in function of its particular geometrical boundaries.

In this project ABAQUS® FEM software is used to study the physical behavior of a pipe under cold bending conditions.

3.5.1 GENERAL SIMULATION STRUCTURE STUDY CASE

To perform a simulation three main steps have to be concluded as can be seen following (*Figure 3.24*):

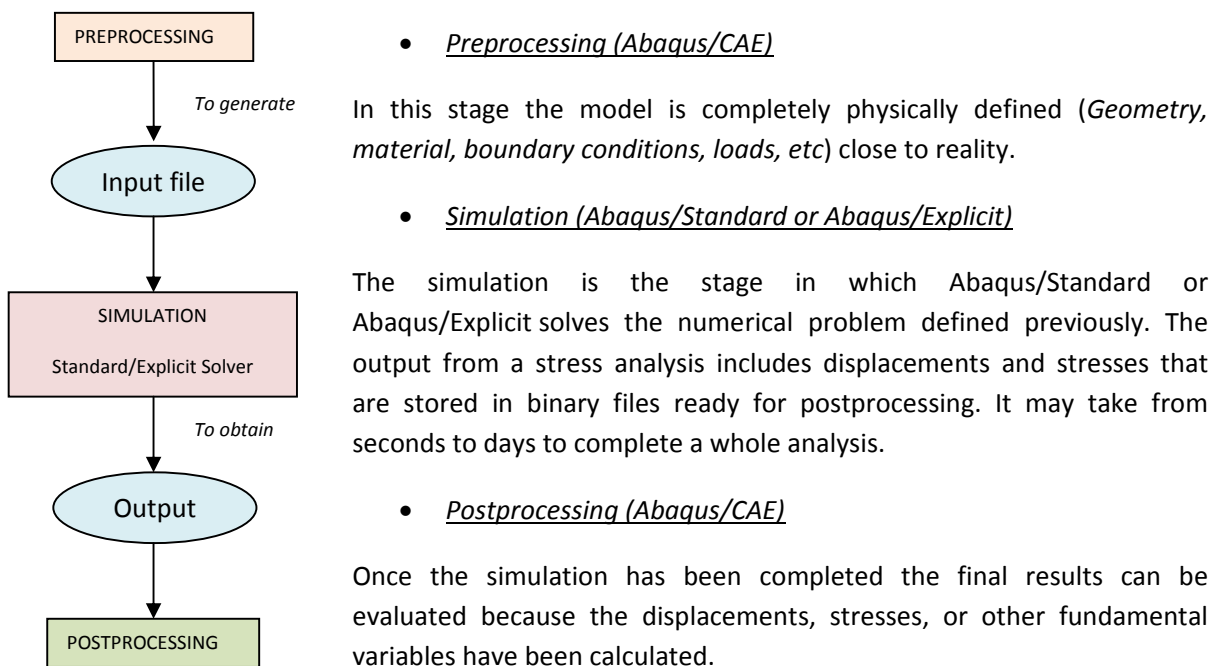


Fig. 3.24 – FEM Simulations Flow Diagram

3.5.1.1 STANDARD VERSUS EXPLICIT SOLVER

Abaqus® Standard is general-purpose analysis computational software that can solve a wide range of linear and nonlinear problems involving the static, dynamic, thermal, and electrical response of components.

For these purposes, solver solves a system of equations implicitly at each solution “increment”, it means must iterate to determine the solution to a nonlinear problem.

The unconditionally stable implicit method will encounter some difficulties when a complicated three-dimensional model is considered. The reasons are as follows:

- As the reduction of the time increment continues causing divergence.
- Local instabilities cause force equilibrium to be difficult to achieve.

Abaqus® Explicit is a special-purpose analysis solver that uses an explicit dynamic finite element formulation. The solver tries to reach a solution forward through time in small time increments without solving a coupled system of equations (***implicit solver***) at each increment. It determine the solution without iterating by explicitly advancing the kinematic state from the previous increment

The explicit techniques are thus introduced to overcome the disadvantages of the implicit method. For the explicit method, the CPU cost is approximately proportional to the size of the finite element model and does not change as dramatically as the implicit method.

The problem of the explicit method is that it is conditionally stable. The stability limit for an explicit operator is that the maximum time increment must be less than a critical value of the smallest transition times for a dilatational wave to cross any element in the mesh.

3.5.1.2 GENERAL SOLVERS SOLUTION DESCRIPTION ^[19]

The implicit procedure uses an automatic increment strategy based on the success rate of a full Newton iterative solution method based:

$$F = m * a$$

(Eq. 24)

Where:

- F : Applied load.
- m : Mass of the object.
- a : Acceleration.

It can be rewrite more complex using constitutional equations and taking into account the nodal displacements as follows:

$$\Delta u^{(i+1)} = \Delta u^{(i)} + K_t^{(-1)} * (F^{(i)} - I^{(i)})$$

(Eq. 25)

Where:

- K_t : Current tangent stiffness matrix.
- I : Internal Force Vector.
- Δu : Increment of displacement.

Implicit dynamic procedure consists step by step in the subsequently analytical steps:

$$M\ddot{u}^{(i+1)} + (1+\alpha)Ku^{(i+1)} - \alpha Ku^{(i)} = F^{(i+1)}$$

(Eq. 26)

Where:

- M : Mass matrix.
- K : Stiffness matrix.
- F : Vector of applied loads.
- u : Displacement vector.

$$u^{(i+1)} = u^{(i)} + \Delta t\dot{u}^{(i)} + \Delta t^2 \left(\left(\frac{1}{2} - \beta \right) \ddot{u}^i + \beta \ddot{u}^{(i+1)} \right)$$

(Eq. 27)

And:

$$\dot{u}^{(i+1)} = \dot{u}^{(i)} + \Delta t \left((1 - \gamma)\ddot{u}^{(i)} + \gamma\ddot{u}^{(i+1)} \right)$$

(Eq. 28)

With:

$$\beta = \frac{1}{4}(1 - \alpha^2), \quad \gamma = \frac{1}{2} - \alpha, \quad \frac{1}{3} \leq \alpha \leq 0$$

Being α , the damping parameter by default -0.05 to remove the high frequency noise without having a significant effect on the meaningful results.

In other hand, the explicit procedure is based on the implementation of an explicit integration rule along with the use of diagonal elements mass matrices. The equation of motion for the body is integred then using an explicit central difference integration rule being stable governed if the time increments satisfy:

$$\Delta t \leq \frac{2}{\omega_{max}}$$

(Eq. 29)

Where

- ω_{max} : Element maximum eigenvalue.

Also the above time increment can be geometrically limited to reach the stability using the following expression:

$$\Delta t = \min\left(\frac{L_e}{C_d}\right)$$

(Eq. 30)

Where:

- L_e : Characteristic element dimension.
- C_d : Effective dilatational wave speed of the material.

Table 3.5, summarizes and compares the main remarkable characteristics of each solver:

Item	Abaqus/Standard	Abaqus/Explicit
Element lib.	Offers an extensive element library.	Offers an extensive library of elements subset of Standard.
Analysis	General and linear perturbation procedures.	General procedures.
Material models	Offers a wide range of material models.	Similar to those available in Abaqus/Standard; a notable difference is that failure material models are allowed.
Contact formulation	Has a robust capability for solving contact problems.	Has a robust contact functionality that readily solves even the most complex contact simulations.
Solution technique	Uses a stiffness-based solution technique that is unconditionally stable.	Uses an explicit integration solution technique that is conditionally stable.
Disk space and memory	Due to the large numbers of iterations possible in an increment, disk space and memory usage can be large.	Disk space and memory usage is typically much smaller than that for Abaqus/Standard.

Table 3.5 – Solvers comparison

3.5.1.3 RIGID AND DEFORMABLE BODIES

To create any FEM simulation, all of the parts playing a role on it are needed to define. For this purpose each part has to be firstly defined like a **rigid body** (*body which moves through space without shape and physical properties change during it*) or **finite element** (*deformable body in function of constitutional equations*).

Rigid bodies are usually used to model the tools and the finites elements are used to discrete the body interested in the study of its physical changes during the simulated process.

Only the finite elements need to be characterized by the following main aspects:

- **Family** – Each element type belongs into a main family elements specifically designed for special purposes. The whole family for stress analysis is showed in the *Figure 3.25*:

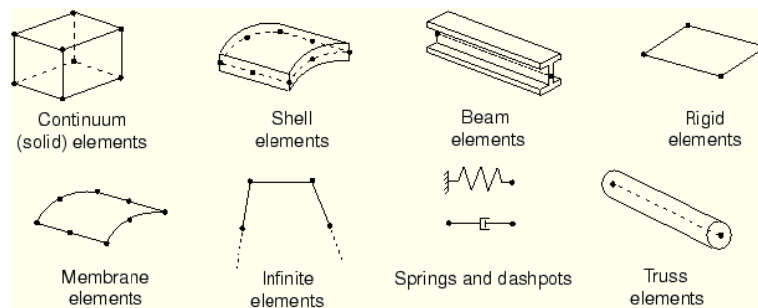


Fig. 3.25 – Solid and shell Family Finite element types

Each one has its own formulation and is preferable to use in specific cases according the problem to solve. For this project solid and shell elements have been studied to carry out the simulations.

- **Degrees Of Freedom** (*directly related to the element family*)

The degrees of freedom (*DOF*) are the fundamental variables calculated during the analysis (*Figure 3.26 & Table 3.6*). For a stress/displacement simulation the 6 degrees of freedom are the translations and rotations at each node. Other DOF can be added like a variable in other cases of study like in thermo-mechanicals cases.

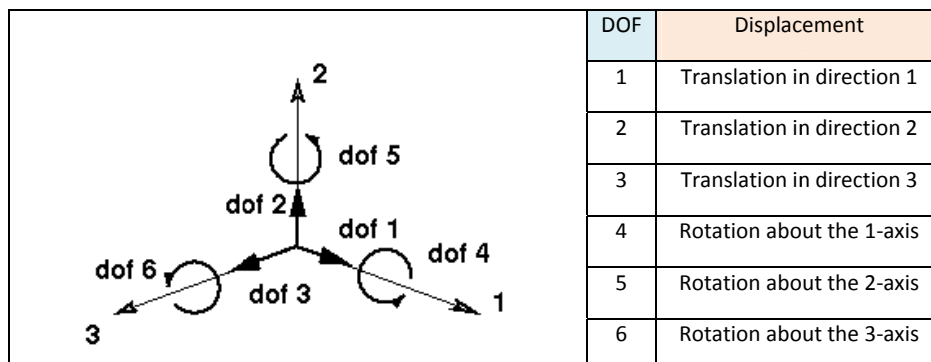


Fig. 3.26 – DOF Diagram & Table 3.6 – DOF

- **Number of nodes**

Displacements, rotations, temperatures, and the other degrees of freedom are calculated only at the nodes of the deformable element depending relate on the element geometry.

The following table shows the finite elements that can be used in each family with its nodal description:



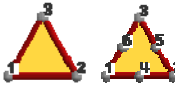
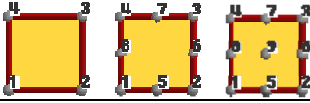
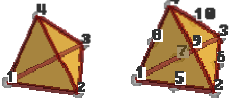

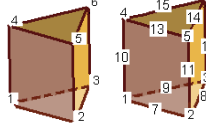
ELEMENT	ELEMENT IMAGE	USE LOCATION
POINT (1 node)		POINTS
LINEAR (2 or 3 nodes)		LINES
TRIANGULAR (3 or 6 nodes)		SHELLS
QUADRATIC (4, 8 or 9 nodes)		SHELLS
TETRAHEDRAL (4 o 10 nodes)		VOLUMES
HEXAHEDRAL (8, 20 o 27 nodes)		VOLUMES
PRISMATICAL (6 o 15 nodes)		VOLUMES

Table 3.7 – Allowable elements and nodes

- **Formulation**

The element's formulation is referring to the mathematical theory used to define the element's behaviour, forces and reactions including displacements.

- **Integration**

Numerical techniques are used to integrate various quantities over the volume of each element. Using Gaussian quadrature for most elements, the software evaluates the material response at each integration point in each element (see Chapters 3.5.1.1 & 3.5.1.2).

3.5.1.4 CONSISTENT SYSTEM UNITS

Abaqus[®] software does not use specific units, however the units must be consistent throughout the model. Regarding the different units systems, is needed to define it in the design simulation phase taking into account this consistent criterion. *Table 3.8* shows the main system units commonly used:

QUANTITY	SI	SI (mm)	US Unit (ft)	US Unit (inch)
Length	m	mm	ft	in
Force	N	N	lbf	lbf
Mass	Kg	Tonne (10 ³ Kg)	Slug	lbf s ² /in
Time	s	s	s	s
Stress	Pa(N/m ²)	MPa(N/mm ²)	lbf/ft ²	psi (lbf/in ²)
Energy	J	mJ (10 ⁻⁰³ J)	ft lbf	in lbf
Density	Kg/m ³	tonne/mm ³	slug/ft ³	lbf s ² /in ⁴

Table 3.8 – Consistent units

3.5.2 PREPROCESSING AND MODEL SET-UP

As described above in *Chapter 3.5.1* the first step is the pre-processing. Following, the FEM simulation model of pipeline bending cold process using ABAQUS[®] is described. Notice that only the main features to set-up the model will be described, not step by step.

The whole simulation consists on several steps as happens in the real process. In order to assess the right results, in this project will be carried out a cold bending pipe procedure to evaluate and check the final results. Subsequently more steps and/or modifications can be included obtaining a final simulation closed to the reality.

3.5.2.1 REAL PROCEDURE

This project is focused primarily in the cold bending process definition, using only mechanical modules of calculation, to ensure the physics of the model, being also one of the objectives of it.

In future works, out of this project objectives, thermo-mechanical module will be added to recreate the whole heat induction bending process^{[20][21]}(see *CD/Bending*), taking into account the applied heat treatment at the same time of the bending process.

Cold bending process consists on placing the whole pipe in the bending machine (*Figure 3.27*). Diminishing the induction coil around the pipe, the pipe passes through the induction coil at a slow, gradual rate as the bending force applied. An exterior arm clamped to the pipe, with only rotational *DOF*, follows the desired bending radius at which the pipe have to be bent. The clamp located in the beginning of the bending radius, remains fixed all the time, to provide the necessary bending moment to deform the pipe.

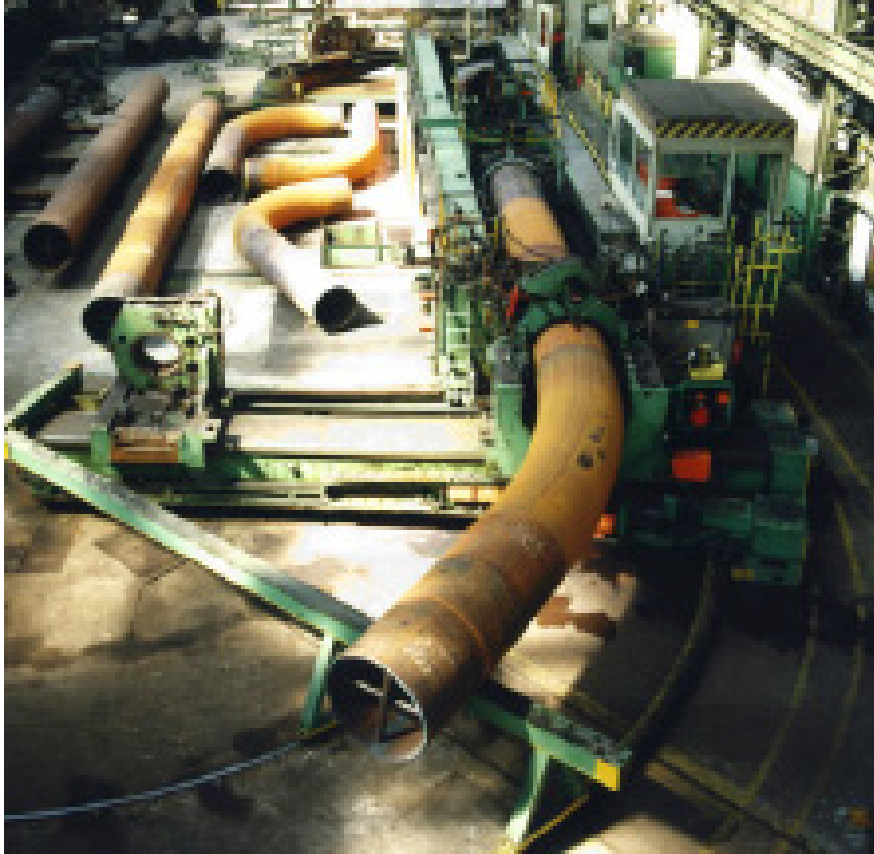


Fig. 3.27 – Heat-induction bending

The real process interested of study, is the case of 5D bend ($48'' \times 24mm$ of *x65 Steel Grade*). Being D the diameter of the pipe, 5D fix the bending radius ($R=6096mm$).

To optimize FEM simulations, the case have been scaled to half all the parameters in order to reduce the computational time costs, obtaining the same results in terms of stresses and deformations with lower times.

The main parts to complete the cold bending process in the real process required are:

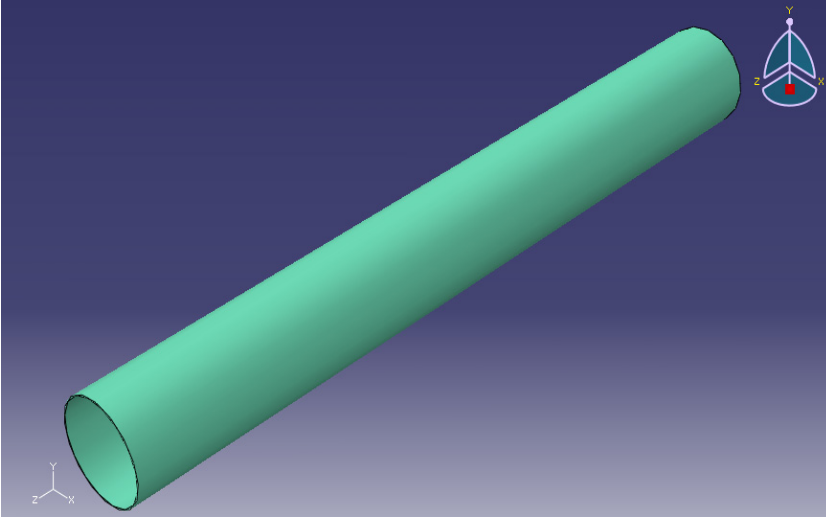
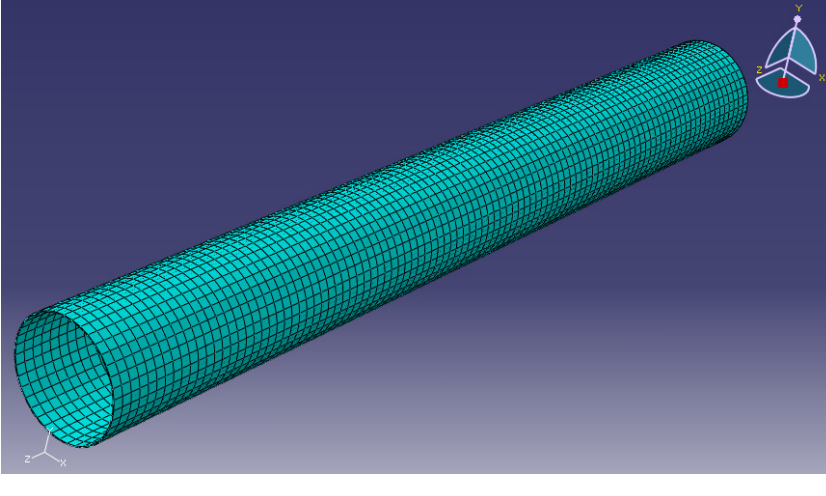
- Pipe desirable to bend.
- Mobile clamp (*with arm*) to provide the bending.
- Fixed Clamp in future the heated area and also the beginning of the bending moment.
- Pusher to reduce or avoid frictions between machine (bending *machine rollings*) and pipe.

3.5.2.2 FEM MODEL SET-UP

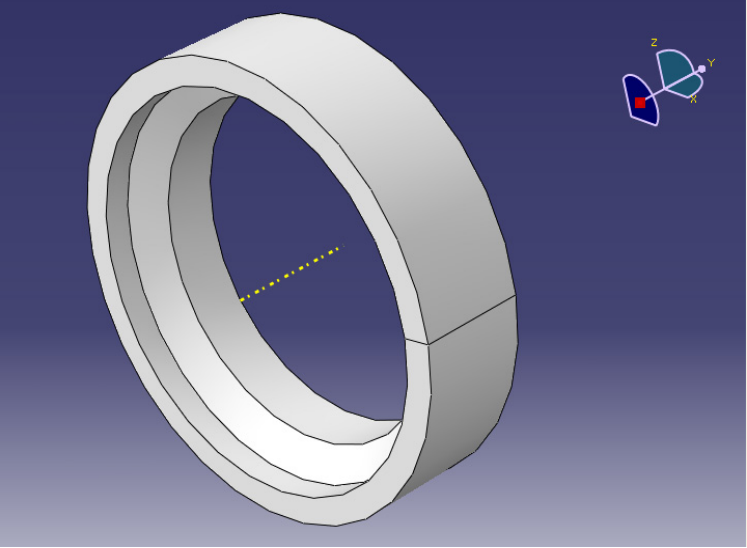
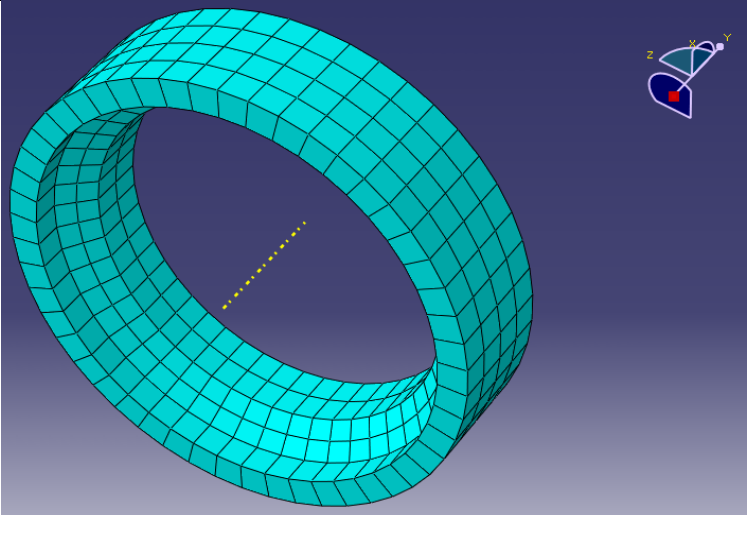
PARTS DESIGN AND MESH MODULE

The 4 parts needed to define FEM definition are following showed and describing design and mesh criteria:

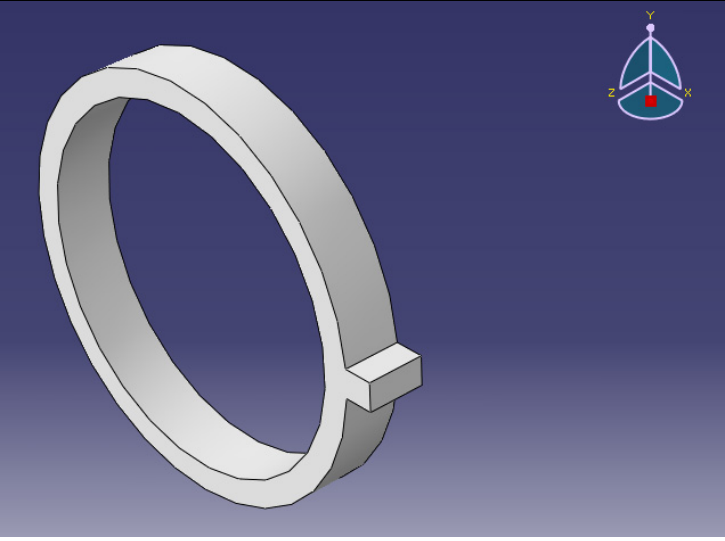
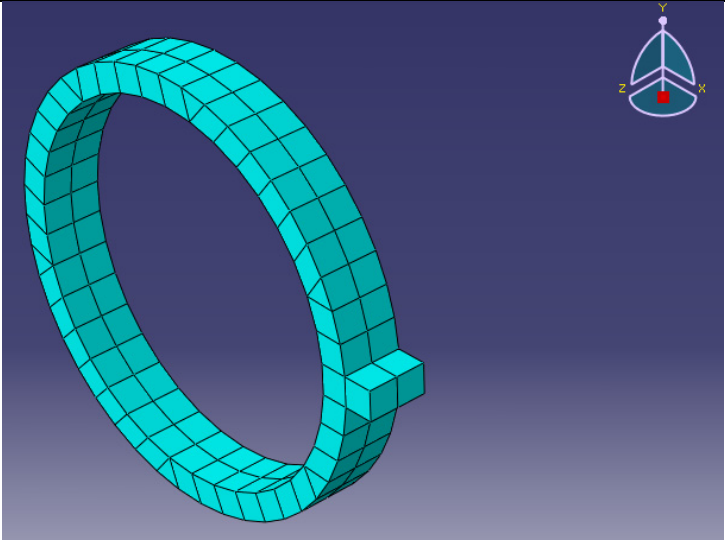
- PART 1 - PIPE

	<p>Type of body</p>	<ul style="list-style-type: none"> • 3D Deformable solid extruded body
	<p>Dimensions</p>	<ul style="list-style-type: none"> • $\varnothing_{\text{external}} = 305\text{mm}$ • $\varnothing_{\text{internal}} = 293\text{mm}$ • Length = 5000mm
	<p>Material Definition</p>	<ul style="list-style-type: none"> • Mass density = $7.85 \times 10^{-9} \text{ Tn/mm}^3$ • Elasticity : Isotropic • E = 210000 GPa • Poisson's ratio = 0.3 • Plasticity : Isotropic • Homogenous
	<p>Mesh criteria</p>	<ul style="list-style-type: none"> • Approximate Global Element Size = 50 mm • Cordal error = 0.1mm • Element type : Hexahedral 8 node full integration
<p>PART DESCRIPTION:</p> <p>Pipe is the deformable part interested to simulate to know deeply the material behavior during the bending and its final mechanical properties.</p>		
<p>COMMENTS:</p> <ul style="list-style-type: none"> • Plasticity is defined using experimental x65 data values from tensile test. Strain = 0.2% correspond Stress = 533.83 MPa 		

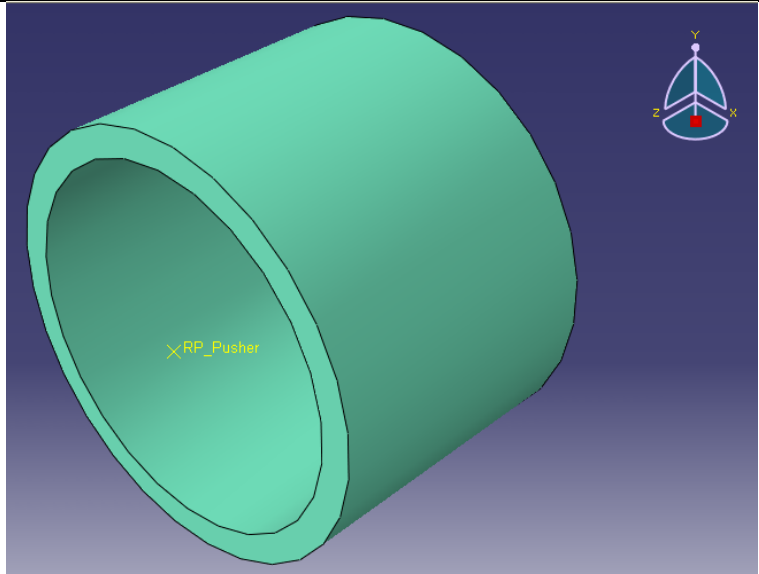
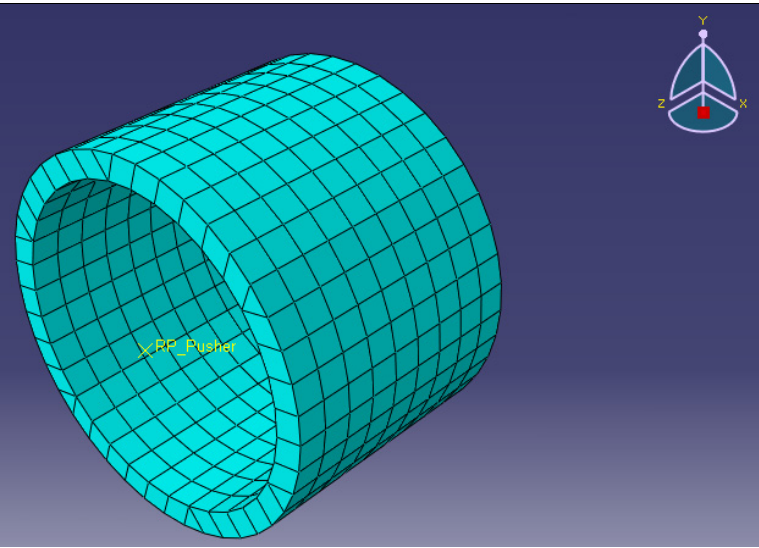
• PART 2 - FIXED CLAMP

	<table border="1"> <tr> <td data-bbox="999 297 1182 405">Type of body</td> <td data-bbox="1182 297 1477 405"> <ul style="list-style-type: none"> • 3D Discrete solid revolved body </td> </tr> <tr> <td data-bbox="999 405 1182 607">Dimensions</td> <td data-bbox="1182 405 1477 607"> <ul style="list-style-type: none"> • $\varnothing_{\text{external}} = 405\text{mm}$ • $\varnothing_{\text{internal}} = 295.05\text{mm}$ • Length = 200mm • Wall inclination = 135° </td> </tr> <tr> <td data-bbox="999 607 1182 943">Material Definition</td> <td data-bbox="1182 607 1477 943"> <ul style="list-style-type: none"> • Mass density = $7.85\text{E-}005 \text{ Tn/mm}^3$ • Elasticity : Isotropic • E = 99999999 GPa • Poisson's ratio = 0.3 • Plasticity : Isotropic • Homogenous </td> </tr> </table>	Type of body	<ul style="list-style-type: none"> • 3D Discrete solid revolved body 	Dimensions	<ul style="list-style-type: none"> • $\varnothing_{\text{external}} = 405\text{mm}$ • $\varnothing_{\text{internal}} = 295.05\text{mm}$ • Length = 200mm • Wall inclination = 135° 	Material Definition	<ul style="list-style-type: none"> • Mass density = $7.85\text{E-}005 \text{ Tn/mm}^3$ • Elasticity : Isotropic • E = 99999999 GPa • Poisson's ratio = 0.3 • Plasticity : Isotropic • Homogenous
Type of body	<ul style="list-style-type: none"> • 3D Discrete solid revolved body 						
Dimensions	<ul style="list-style-type: none"> • $\varnothing_{\text{external}} = 405\text{mm}$ • $\varnothing_{\text{internal}} = 295.05\text{mm}$ • Length = 200mm • Wall inclination = 135° 						
Material Definition	<ul style="list-style-type: none"> • Mass density = $7.85\text{E-}005 \text{ Tn/mm}^3$ • Elasticity : Isotropic • E = 99999999 GPa • Poisson's ratio = 0.3 • Plasticity : Isotropic • Homogenous 						
	<table border="1"> <tr> <td data-bbox="999 943 1182 1496">Mesh criteria</td> <td data-bbox="1182 943 1477 1496"> <ul style="list-style-type: none"> • Approximate Global Size = 27 mm • Cordal error = 0.1mm • Element type : Hexahedral 8 node full integration </td> </tr> </table>	Mesh criteria	<ul style="list-style-type: none"> • Approximate Global Size = 27 mm • Cordal error = 0.1mm • Element type : Hexahedral 8 node full integration 				
Mesh criteria	<ul style="list-style-type: none"> • Approximate Global Size = 27 mm • Cordal error = 0.1mm • Element type : Hexahedral 8 node full integration 						
<p>DESCRIPTION:</p> <p>Fixed clamp is the part where the pipe has to flow during the bending and in conjunction with the mobile clamp, and due this parte have each 6 DOF constrained like an encastre ($U1=U2=U3=UR1=UR2=UR3=0$), providing the initial bending support.</p>							
<p>COMMENTS:</p> <ul style="list-style-type: none"> • Material was scale-up to recreate a solid discrete rigid body due software forbidden capabilities to create the model (contact conditions and also constrain and interactions between parts). • Density has been increased to help avoiding deformations, indeed, the rest of constants. • Plasticity defined using experimental x65 data values from tensile test. Strain = 0.0% correspond Stress = 999999999MPa. • Offset of 0.05mm is needed in the inner diameter to avoid initial distortions due to overclosures. 							

• PART 3 - MOBILE CLAMP

	<p>Type of body</p> <ul style="list-style-type: none"> • 3D Discrete solid extruded body
	<p>Dimensions</p> <ul style="list-style-type: none"> • \varnothingexternal = 405mm • \varnothinginternal = 295.05mm • Length = 100mm
	<p>Material Definition</p> <ul style="list-style-type: none"> • Mass density = 7.85E-010 Tn/mm³ • Elasticity : Isotropic • E = 99999999 GPa • Poisson's ratio = 0.3 • Plasticity : Isotropic • Homogenous
	<p>Mesh criteria</p> <ul style="list-style-type: none"> • Approximate Global Size = 50 mm • Cordal error = 0.1mm • Element type : Hexahedral 8 node full integration
<p>DESCRIPTION:</p> <p>Mobile clamp is the part which will governate the rotational movement followed by the pipe to apply the bending.</p> <p>To describe the rotational movement, a reference point has been created at 1500mm from the center in X direction, being the axial reference, and the bending radius definition.</p>	
<p>COMMENTS:</p> <ul style="list-style-type: none"> • Material was scale-up to recreate a solid discrete rigid body due software forbidden capabilities to create the model (<i>contact conditions and also constrain and interactions between parts</i>). • Density has been decreased to avoid inertial contributions. • Plasticity defined using experimental x65 data values from tensile test. Strain = 0.0% correspond Stress = 9999999999MPa. • Offset of 0.05mm is needed in the inner diameter to avoid initial distortions due to overclosures. 	

• PART 4 - PUSHER

	<p>Type of body</p> <ul style="list-style-type: none"> • 3D Discrete solid extruded body
	<p>Dimensions</p> <ul style="list-style-type: none"> • $\varnothing_{\text{external}} = 405\text{mm}$ • $\varnothing_{\text{internal}} = 295.05\text{mm}$ • Length = 400mm
	<p>Material Definition</p> <ul style="list-style-type: none"> • Mass density = $7.85 \times 10^{-6} \text{ Tn/mm}^3$ • Elasticity : Isotropic • E = 99999999 GPa • Poisson's ratio = 0.3 • Plasticity : Isotropic • Homogenous
	<p>Mesh criteria</p> <ul style="list-style-type: none"> • Approximate Global Size = 50 mm • Cordal error = 0.1mm • Element type : Hexahedral 8 node full integration
<p>DESCRIPTION:</p> <p>Pusher is the part which will help to avoid and minimize flexor moments contributions in the bending process in the tail of the pipe describing only a linear movement.</p>	
<p>COMMENTS:</p> <ul style="list-style-type: none"> • Material was scale-up to recreate a solid discrete rigid body due software forbidden capabilities to create the model (<i>contact conditions and also constrain and interactions between parts</i>). • Density has been decreased to minimize inertial contributions and being a linear support guide for the tail of the pipe imposing this movement and avoiding any other resulting movement due the bending moments and stresses. • Plasticity defined using experimental x65 data values from tensile test. Strain = 0.0% correspond Stress = 999999999MPa. • Offset of 0.05mm is needed in the inner diameter to avoid initial distortions due to overclosures. 	

PARTS ASSEMBLY MODULE

Once the different parts have been designed and modelled, each one needs to be placed in the virtual space, taking into account the geometrical conditions and real constraints that are also required in the initial FEM step. For this purpose, using the assembly module, one or several instances of each part is created, rotated and/or translated to its correct position in order to locate it with respect to each other.

The assembled model is presented below (*Figure 3.28*):

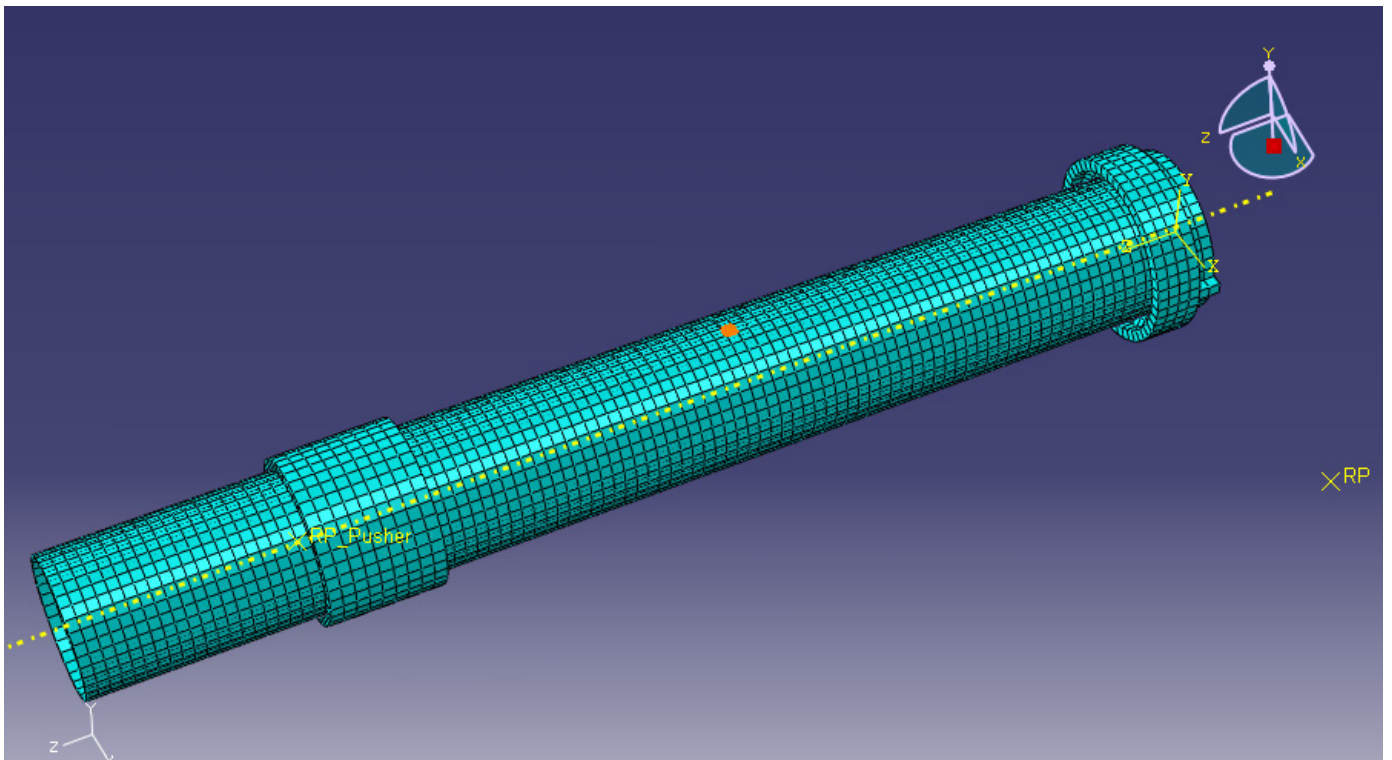


Fig. 3.28 – Assembled FEM model

The position constraints used in this model have been:

- Coaxial – To place coaxially the pusher and both clamps regarding the pipe.
- Face to face – To place each part in trough the Z pipe axis in the correct length position:
 - Pusher – Have been placed at 1000mm from the rear face of the pipe.
 - Mobile clamp – Have been placed at 0mm from the front face of the pipe.
 - Fixed clamp – Have been placed at 0mm subsequently from the mobile clamp part.

STEPS MODULE

FEM simulations can be divided into different steps, depending on the physical process wanted to simulate.

In the actual model, the cold bending process will be simulated creating 2 different steps:

- STEP 1 : Dynamic explicit step – Named “Gravity” during this step, gravity force is applied to ensure the proper contacts of each part before proceeding the bending. The step time have to be enough to affects and move each part in case of unconstrained parts, that can conclude in a model failure due the bad constrain definition.

The defined time step is: 0.001s

- STEP 2: Dynamic explicit step – Named “Bending” during this step, all the movements are defined to carry out the bending FEM simulation process.

This time is calculated in function of the linear velocity needed to describe a specific radius of the pipe bending, according the following equation:

$$t_{simulation} = \frac{\varphi}{\omega} \quad (Eq. 31)$$

Where:

- φ : Angular rotational displacement [rad].
- ω : Angular velocity [rad/s].

Previously to the performance of this simulation, some calculations have to be taking into account. Firstly a linear velocity of 0.45 m/s (450mm/s) for the pipe has been defined.

Using this value, and knowing that the radius of bending is R=1500mm, the angular velocity is calculated obtaining $\omega = 0.3$ rad/s.

The maximum angular rotational displacement φ , discriminating the amplitude effect, is 1.53 rad (87.6°).

And finally, the time needed for the simulation can be solved, using the equation 31:

$$t_{simulation} = \frac{1.53}{0.3} = 5.1s$$

INTERACTIONS

Although the parts have been assembled, more information is needed for the software to define the interactions between the different meshed surfaces during the simulation. To define it master-slave contact pairs have to be defined for all the surfaces in contact with each other.

Abaqus provides two algorithms to model contact interactions: The **general contact interactions** allow defining contact between many or all regions of the model with a single interaction and **surface-to-surface contact interactions** describe contact between two deformable surfaces or between a deformable surface and a rigid surface.

In this model, surface-to-surface contact definition has been used. It requires the definition of all the surfaces in contact with each other (Figure 3.29). The master and the slave surfaces should be defined for each interaction set, being considered the fixed clamp inner surface as the “**master surface**” while considering the outer pipe surface as the “**slave surface**”.

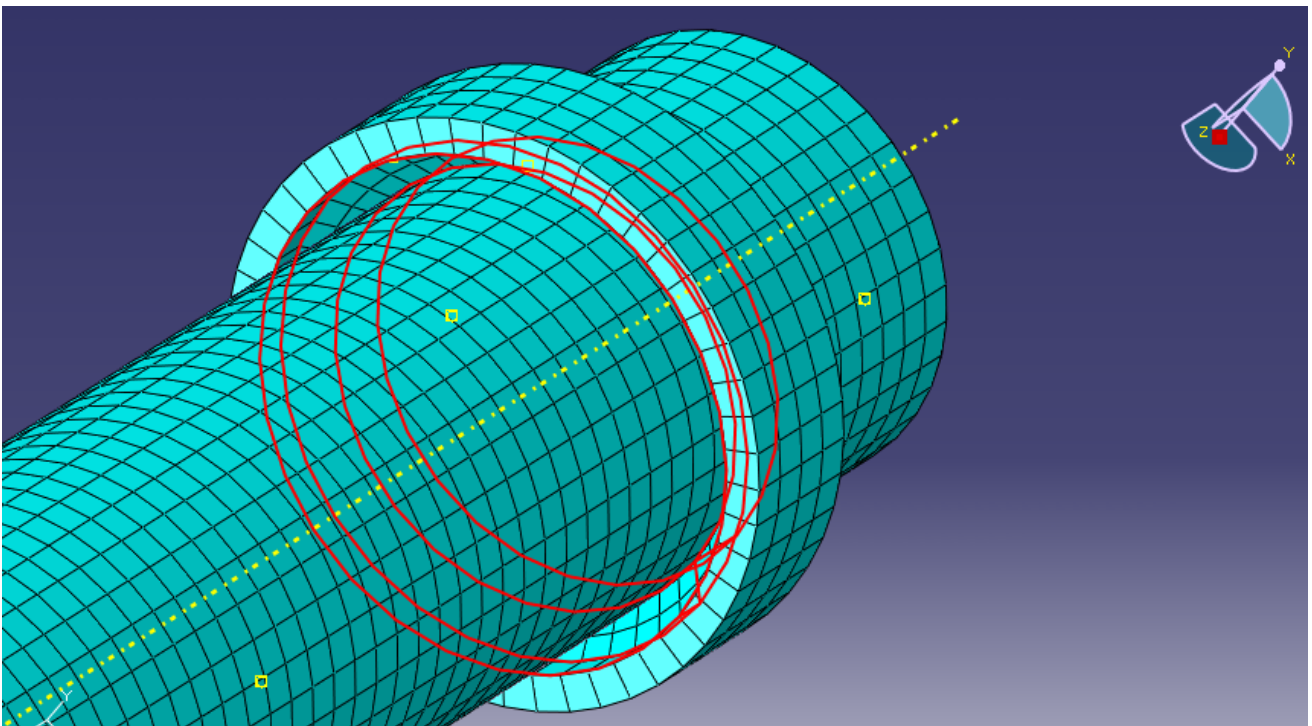


Fig. 3.29 – Assembled FEM model

Also the kinematic constrain formulation has to be applied using “*kinematic contact*” or “*penalty contact*”:

- Kinematic contact - First advances the kinematic state of the model into a predicted configuration without considering the contact conditions. After, the slave nodes in the predicted configuration that are penetrating the master surfaces are defined and the depth of each slave node’s penetration, the mass associated with it, and the time increment are used to calculate the resisting force required to oppose penetration
- The penalty contact algorithm searches for slave node penetrations in the current configuration. Contact forces that are a function of the penetration distance are applied to the slave nodes to oppose the penetration, while equal and opposite forces act on the master surface at the penetration point

The penalty contact algorithm results in less severe enforcement of contact constraints than the kinematic contact algorithm, but the penalty algorithm allows for treatment of more general types of contact, being used for this model. Also, a very important aspect is that Coulomb friction is defined like $\mu=0$ in this contact pair, to minimize the pipe distortion due frictional effects once is flowing through the fixed clamp.

CONSTRAINS

Despite interactions in the whole contact surfaces is the commonly way to perform a FEM model, in this case several contact problems have appeared difficulting it.

Due the intrinsical characteristics of the simulation, however, an alternative way has been defined to provide a successfully method to define the rest of the contacts using constrains options.

MOBILE CLAMP

To describe properly and control the mobile clamp rotational movement, a reference point with an offset of the desired bending radius ($R=1500mm$) respect the axial pipe coordinates (Y axis) straight on the X axis, has been created as can be see following (Figure 3.30):

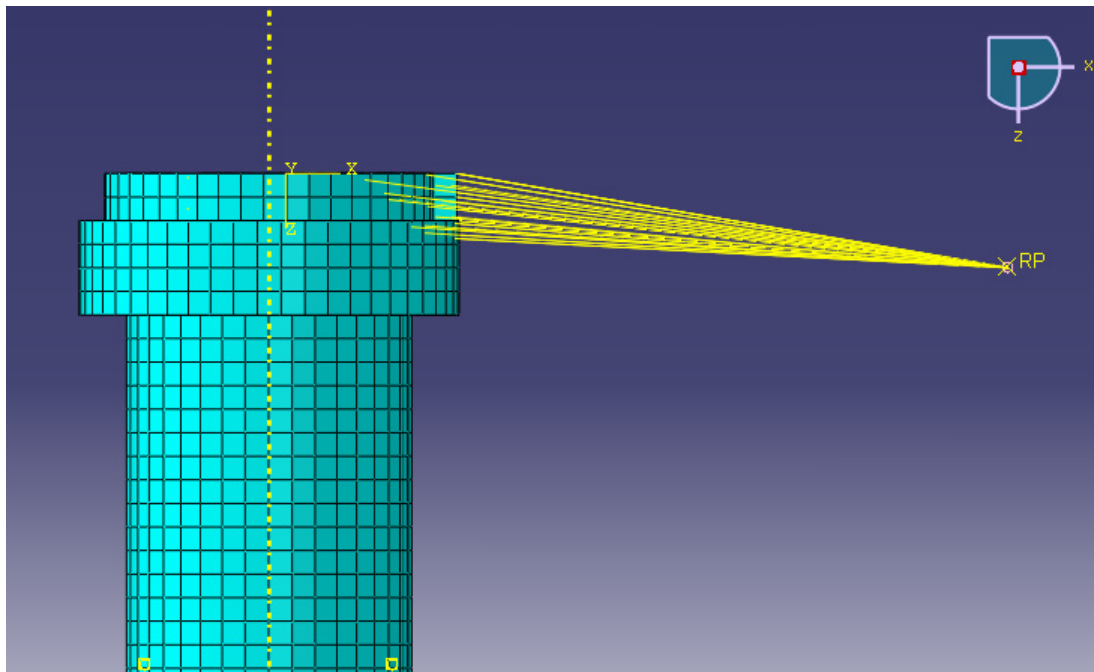


Fig. 3.30 – Mobile Clamp Constrains

As can be seen in this reference point (RP), the angular velocity **DOF** (VR2-Red arrow in figure 3.29) is applied, so a coupling constrain involving RP and all the nodes from the mesh of the mobile clamp is applied forcing all its nodes to follow exactly the same movement of the RP, defining the bending rotational movement.

This rotational movement only affects the mobile clamp, regarding that no interaction between the mobile clamp and the pipe has been yet create. For this reason another constrain is required to “weld” the nodes of the inner clamp surface and the pipe outer surface.

Figure 3.31 shows a tied constrain between the surfaces which is defined recreating a “weld” condition and guarantying that pipe is following the movement of the mobile clamp.

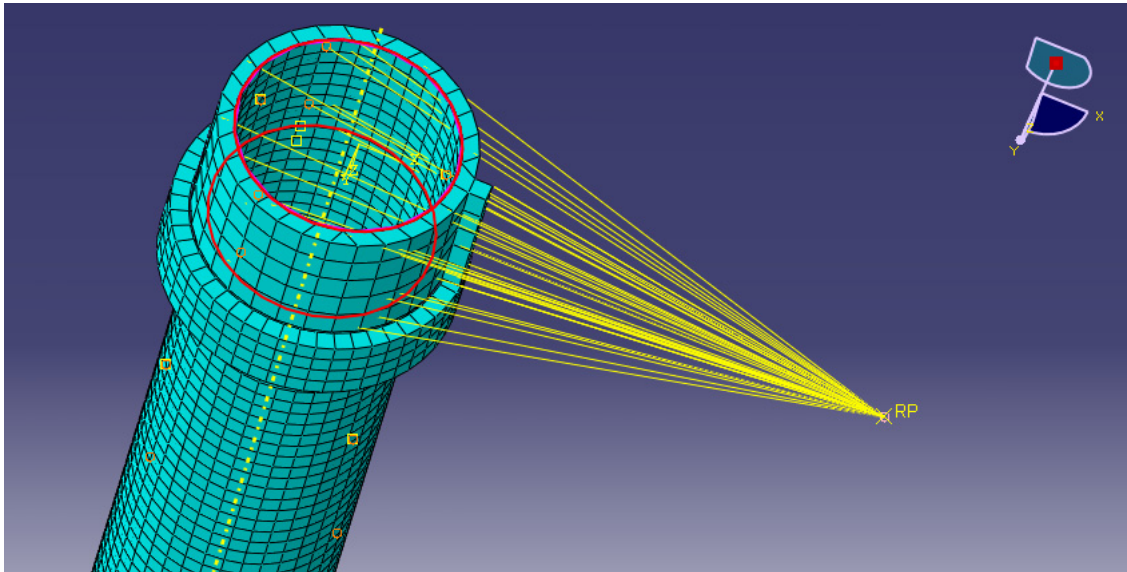


Fig. 3.31 – Mobile Clamp & Pipe Tie and Coupling Constrains

PUSHER

Same procedure is used to define the linear translational pusher movement (Figure 3.32), creating firstly its own RP and after a coupling constrain between RP and the nodes finishing with another constrain to “weld” coupling both interacting surfaces.

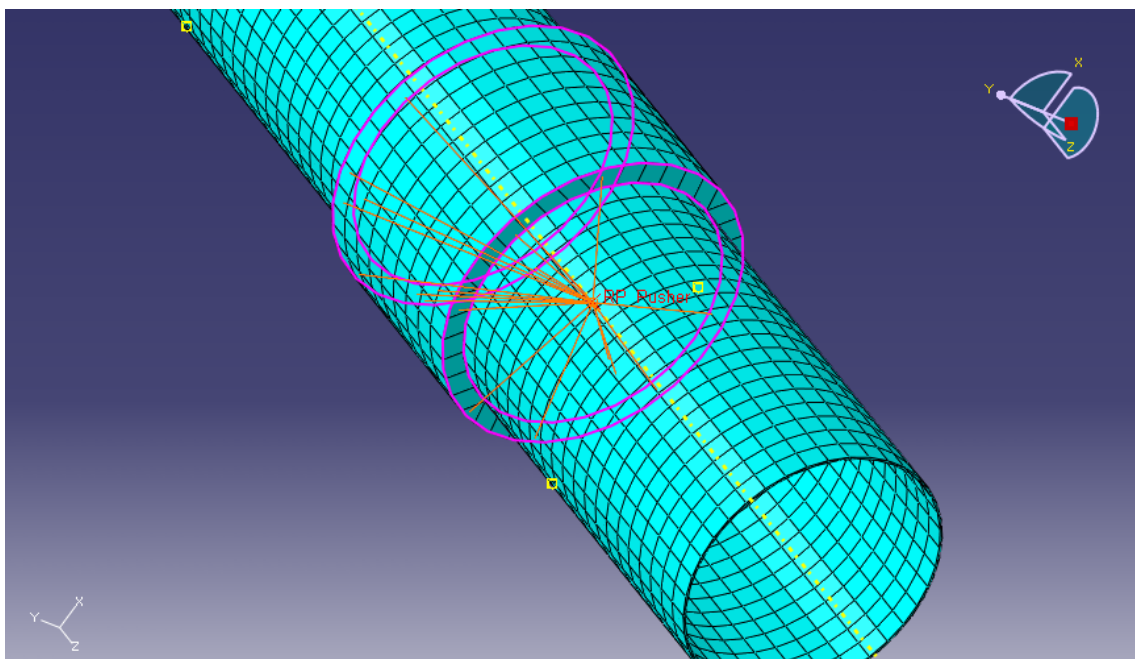


Fig. 3.32 – Pusher & Pipe Tie and Coupling Constrains

AMPLITUDE ASSIGNMENTS

In order to avoid accelerations problems, product to change the velocity (*from 0 mm/s until X mm/s*) value in the same time step and due the partial derivation used by the solver for each increment of time, the solver can reach an infinite or very high final value, which may lead to unexpected time and force instabilities.

To avoid the instabilities, is very helpfully the application of an initial smooth step within the main step in gravity as in bending.

This initial smooth step is applied where the velocity increases gradually till the required bending velocity and then, a constant velocity step is employed. Finally, a deceleration step is applied towards the end of the bending process until a velocity equal to zero is reached.

4 RESULTS AND DISCUSSION

4.1 SAMPLING AND COATING RECREATION

The recorded real temperature evolution of the samples during the coating simulation process in the furnace is following plotted (Figure 4. 1 & Figure 4. 2):

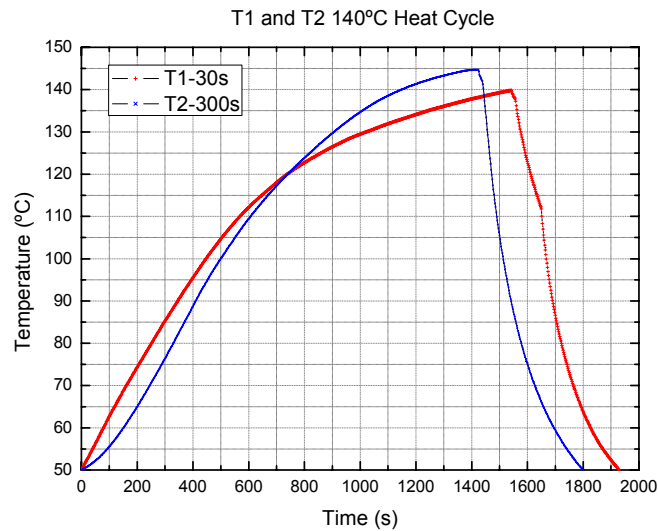


Fig. 4. 1 – T1 and T2 Heat Treatment

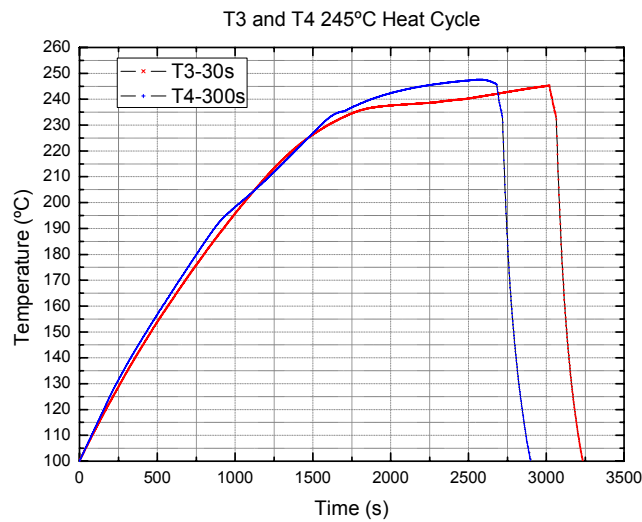


Fig. 4. 2 – T3 and T4 Heat Treatment

Due the nature of the furnace, the maximum value of temperature that can be reached is 245°C, and taking into account the heating power high values of time are needed to reach the desired temperature in the samples longer than the applied in the coating processes if quenched is applied (Table 1.4 & CD/COATINGS).

4.2 TENSILE TEST

The tensile test results obtained from the tensile test are appointed in *Table 4.1* followed of the results in *Table 4.2* and *Table 4.3*. (See Chapter 3.2.1 for a complete explanation. All experimental data and the obtained curves can be found in CD/TENSILE TESTS).

Description	Unit	Symbol	Remarks
<i>E-modulus</i>	GPa	E	Measured E modulus between 50 and 100 MPa.
<i>Yield Stress (0.2%)</i>	MPa	Rp0.2	Yield Stress at 0.2% remaining deformation.
<i>Rt0.5</i>	MPa	Rt0.5	Proof strength, total extension 0.5%.
<i>Maximum Stress (σ_{YS})</i>	MPa	Rm	EN 10002-standard.
<i>Homogenous Strain</i>	%	Ag	Technical strains at Rm.
<i>Rupture Strain</i>	%	A25	Rupture Strain.
<i>Proportional Elongation at rupture</i>	%	A _{prop}	% ratio between elongation and initial length.
<i>Fracture location</i>			Inside - valid measurement. Sensor arm break - measurement unsure. Outside - invalid measurement.
<i>Resilience</i>	MPa	U_R	Area Measurement until determined Rp0.2.
<i>Toughness</i>	$\frac{J}{m^3}$	T _o	Total Area Measurement.
<i>Strain Hardening</i>		n	Measured until $\epsilon=1$.

For further clarification of the used terminology please refer to the standard EN10002.

Table 4. 1 - Clarification of symbols

Sample ID	*E	Rp 0.2	Rt 0.5	Rm	Ag	A25	Aprop	BP
BASE-1	208 ^{±3}	463 ^{±5}	487 ^{±5}	610 ^{±1}	8.1 ^{±0.1}	28.5 ^{±0.2}	19.3 ^{±0.1}	Break within
BASE-2	213 ^{±3}	462 ^{±5}	484 ^{±5}	610 ^{±1}	8.2 ^{±0.1}	28.8 ^{±0.2}	19.5 ^{±0.1}	Break within
BASE-3	204 ^{±3}	467 ^{±5}	487 ^{±5}	611 ^{±1}	8.3 ^{±0.1}	28.3 ^{±0.2}	19.2 ^{±0.1}	Break within
T1-1	217 ^{±4}	476 ^{±6}	497 ^{±6}	610 ^{±1}	7.8 ^{±0.1}	28.0 ^{±0.2}	19.0 ^{±0.2}	Break within
T1-2	227 ^{±4}	462 ^{±6}	489 ^{±6}	610 ^{±1}	8.1 ^{±0.1}	28.7 ^{±0.2}	19.5 ^{±0.2}	Break within
T1-3	221 ^{±4}	470 ^{±6}	493 ^{±6}	609 ^{±1}	8.0 ^{±0.1}	28.5 ^{±0.2}	19.3 ^{±0.2}	Break within
T2-1	213 ^{±2}	468 ^{±4}	496 ^{±4}	607 ^{±1}	8.1 ^{±0.2}	27.0 ^{±0.4}	18.3 ^{±0.5}	Break within
T2-2	237 ^{±2}	463 ^{±4}	494 ^{±4}	613 ^{±1}	7.8 ^{±0.2}	28.0 ^{±0.4}	19.0 ^{±0.5}	Break within
T2-3	213 ^{±2}	469 ^{±4}	491 ^{±4}	614 ^{±1}	7.7 ^{±0.2}	24.9 ^{±0.4}	16.9 ^{±0.5}	Break within
T3-1	224 ^{±5}	559 ^{±3}	562 ^{±3}	629 ^{±1}	6.7 ^{±0.1}	26.9 ^{±0.3}	18.2 ^{±0.2}	Break within
T3-2	226 ^{±5}	562 ^{±3}	565 ^{±3}	632 ^{±1}	6.7 ^{±0.1}	26.8 ^{±0.3}	18.2 ^{±0.2}	Break within
T3-3	221 ^{±5}	557 ^{±3}	559 ^{±3}	629 ^{±1}	6.7 ^{±0.1}	25.1 ^{±0.3}	17.0 ^{±0.2}	Break within
T4-1	227 ^{±3}	560 ^{±6}	564 ^{±6}	632 ^{±1}	6.2 ^{±0.1}	25.2 ^{±0.2}	17.1 ^{±0.1}	Break within
T4-2	236 ^{±3}	559 ^{±6}	562 ^{±6}	631 ^{±1}	6.8 ^{±0.1}	26.0 ^{±0.2}	17.6 ^{±0.1}	Break within
T4-3	244 ^{±3}	560 ^{±6}	564 ^{±6}	631 ^{±1}	6.7 ^{±0.1}	26.2 ^{±0.2}	17.8 ^{±0.1}	Break within

Table 4. 2 - Tensile test results of Stress and Strains

* The E-modulus is calculated between 50 and 150 MPa.

Following a comparison of the average tensile test results is following plotted (Figure 4. 3 & Figure 4. 4):

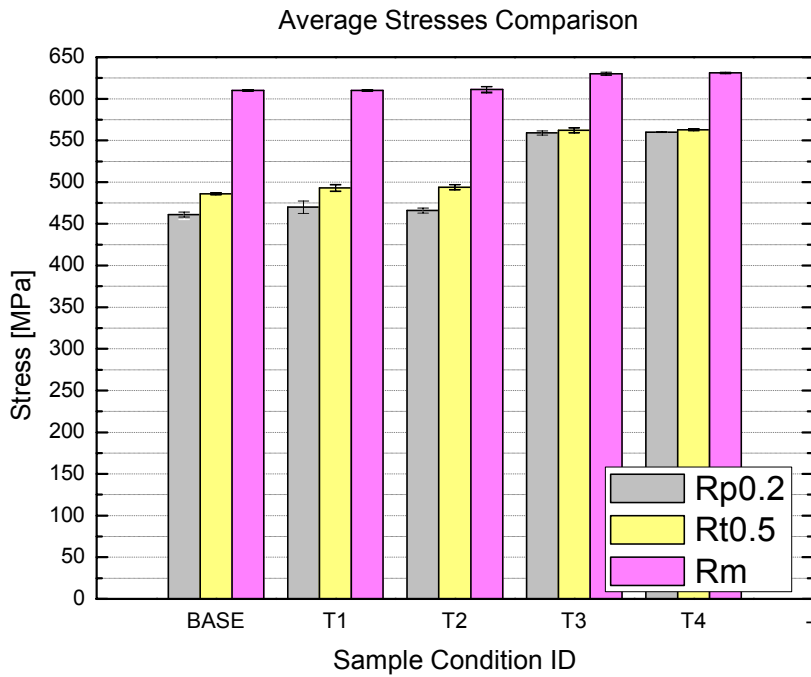


Fig. 4. 3 – Average Stresses Comparison

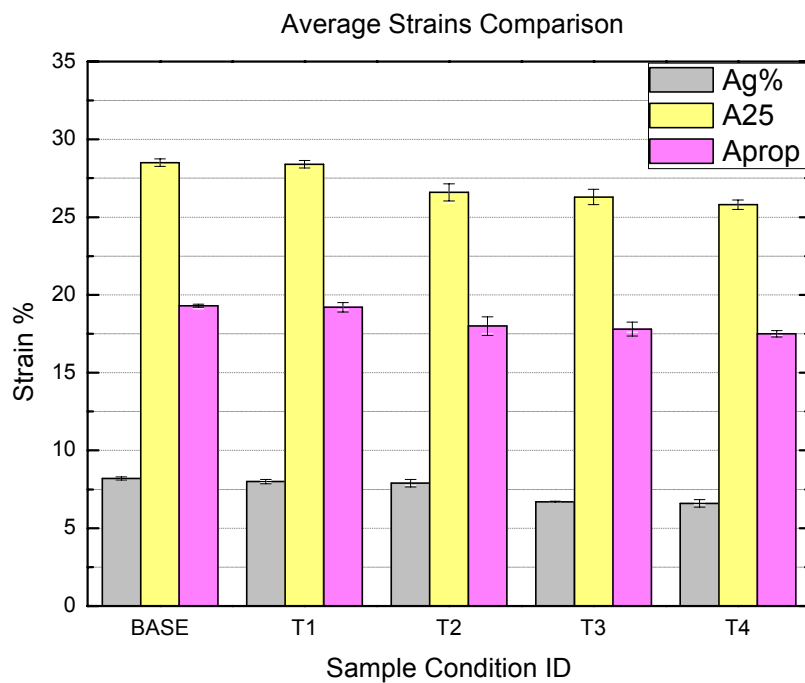


Fig. 4. 4 – Average Strains Comparison

Looking stresses (*Table 4.2 and Figure 4.3*), heated simulations T1 and T2 do not exhibit any significant change in stress compared to the base material. Heated simulations T3 and T4 however show significant higher ultimate tensile strength (*R_m*) and yield strength (*R_{p0.2}* and *R_{t0.5}*).

Taking into account that long times have been needed to reach the desired temperature, as can be seen in *Figures 4.1 & 4.2*, the time has no influence in the results, being the temperature the main factor that alters the mechanical properties.

The E has no significant change in any case, because of the ratio that reflect (stress-strain slope in the elastic region) is almost the same despite tends to increase in T3 and T4 heated simulations. Taking into account that the values have been obtained using a range of stress between 50 and 150 MPa, is means that the higher slope the lower strain is obtained.

On the other hand, *Figure 4.4*, shows clearly that the rupture strain (*A₂₅*) is lower for simulations T3 and T4 than for the Base material and both T1 and T2 heated simulations.

The ductility (*A_{PROP}*) tends to decrease in heated simulations T3 and T4 compared to Base material, which has the greater values, and also with T1 and T2 heated simulations, which have closed lower values than the last one.

Sample ID	U _R	To	n	Rt0.5/Rm
BASE-1	1.025 ^{±0.010}	155.8 ^{±0.6}	0.61	0.79 ^{±0.30}
BASE-2	0.964 ^{±0.010}	157.2 ^{±0.6}	0.61	0.79 ^{±0.30}
BASE-3	0.969 ^{±0.010}	154.7 ^{±0.6}	0.61	0.79 ^{±0.30}
T1-1	1.008 ^{±0.015}	152.3 ^{±0.4}	0.65	0.81 ^{±0.35}
T1-2	1.005 ^{±0.015}	156.9 ^{±0.4}	0.63	0.80 ^{±0.35}
T1-3	0.922 ^{±0.015}	155.2 ^{±0.4}	0.57	0.81 ^{±0.35}
T2-1	0.915 ^{±0.018}	146.8 ^{±0.2}	0.39	0.82 ^{±0.25}
T2-2	0.948 ^{±0.018}	153.7 ^{±0.2}	0.62	0.81 ^{±0.25}
T2-3	0.981 ^{±0.018}	137.5 ^{±0.2}	0.68	0.79 ^{±0.25}
T3-1	1.277 ^{±0.014}	150.5 ^{±0.8}	0.72	0.89 ^{±0.20}
T3-2	1.258 ^{±0.014}	149.0 ^{±0.8}	0.66	0.89 ^{±0.20}
T3-3	1.237 ^{±0.014}	139.9 ^{±0.8}	0.62	0.88 ^{±0.20}
T4-1	1.254 ^{±0.021}	140.0 ^{±0.4}	0.61	0.89 ^{±0.35}
T4-2	1.254 ^{±0.021}	146.0 ^{±0.4}	0.72	0.89 ^{±0.35}
T4-3	1.228 ^{±0.021}	148.0 ^{±0.4}	0.72	0.89 ^{±0.35}

Table 4. 3 – Extracted results from Tensile Test

In *Table 4.3* the values of the U_R are higher than the base material and T1 and T2 heated simulations so more energy can be absorbed in the elastic region. In other hand, although do not have significant changes, tends to decrease in T3 and T4 heated simulations. It means that the total area under the stress-strain curve is less due the higher stress values and lower A₂₅ values.

The n obtained values from the total of tested samples are higher than the standard values for x65 steel grade (between 0.40 and 0.45). As explained in Chapter 3.2.1 the higher the value is the higher is the applied strain in the material. These higher values show that in the UOE process, the tested area is prestrained.

Prestrain means introduce plasticity in the material, so the $Rp0.2$ is passed. Regarding the UOE process (see Chapter 1.3.3)^[3] in the second process step forms the U, on the down of the U, the material need to resist the stresses once the material is drawing and conforming the U adapting to the punch geometry. In a previous FEM simulation of the UOE process the U step forming was simulated as can be seen in the following sequences (Figure 4. 5):

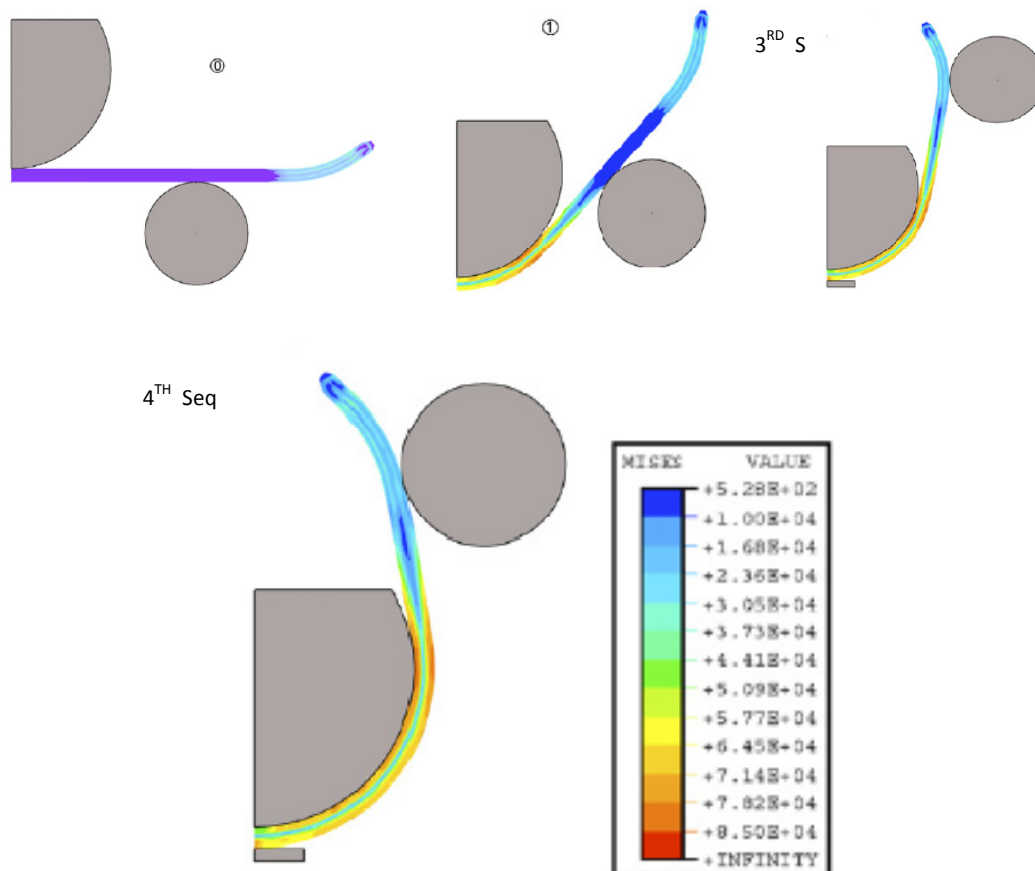


Fig. 4. 5 – FEM U Step Process Sequence

As can be seen in 4th sequence, the Von-Mises stresses reach values up to 70000psi (482MPa) approximately, so the material has been deformed plastically and n value is higher than standard values for x65 steel grade.

It is important to notice, that the UOE process begins using plates of steel. These plates are also Thermo-Mechanically Cooled Processed (TMCP) in order to control the mechanical properties taking into account the mainly grain boundary preferably misorientation control the grain size and the steel constituents such as Acicular Ferrite (AF), Granular Bainite (GB), Martensite-Austenite (MA), etc. that is strongly dependent of the steel grade. As the steel plates are finally laminated in TMCP, have been demonstrated different mechanical properties comparing the longitudinal direction versus the transverse direction. Despite several research projects are also studying this effects, nowadays all of them reflects that the worst mechanical properties are in the transverse direction and strain hardening could be summed being, then not only UOE process the single way to introduce strain.

Pipe steels have also different chemical constituents, and once the steel is melted and cooled, the hardening can increase due the precipitation of carbides, nitrides, etc. which remains pinned in the ferritic matrix of the steel. Also, the strain applied in the UOE process increases the number of dislocations in the material because of the relative lattice movement of the grains.

The temperatures applied in the simulated heat treatment are so far from the recrystallization temperatures of the steels, typically $0.4T_{\text{MELTING}}$ (above 550°C), and it means that the material has not enough energy to create new equiaxial grains explaining the reason of the decrease in the strain rates showed in *Table 4.2* and *Figure 4.4*.

In other hand, the greater value of heat is enough to provide energy to unpinned some of dislocations, increasing the mechanical properties ($Rp0.2$ and $Rt0.5$) as appear in the *Table 4.2* and *Figure 4.3*. Due the long time needed to reach the temperature using this furnace, any significant difference between T3 and T4 heated simulations appear.

Finally, in the *Table 4.3* a ratio between $Rt0.5/Rm$ is presented. This ratio is very important in pipelines, defined also in the Standard API 5L. This value is very important in the design criteria of the pipelines because have a significant relation with the buckling in pipes. As higher is the value, less is the possibility of buckling failure and longer the length of the pipe depending on the over collapse pressure. According to the API definitions, minimum values of 0.8 guaranties high standards of applications.

Due the increase of the mechanical properties, in T3 and T4 heated simulations, this ratio is increased.

4.3 HEAT TRANSFERS IN CHARPY V_NOTCH TEST

4.3.1 ANALYTICAL PROCEDURE

For analytical procedure, has been needed to find and extrapolate some values of different constants and apply them into the required equations to obtain the values of convective factor h .

The data treatment and results will be presented in the *CD/CSTT/CSTT.xls*.

The analytical procedure will be focused in the two mechanisms described above, natural and forced convection, due to while the Charpy experimental test, the sample is firstly homogeneously cooled into a fridge, and then the sample is picked out and placed into the test Charpy machine. During this procedure is considered that:

- First stage – Forced convection is acting because the sample is picked and placed in the test machine. In this stage a constant velocity of 2m/s is assumed during 5 seconds.
- Second stage – Natural convection is acting because the sample has been placed in the machine, and remains waiting for the hammer impact. Initially is assumed that the contact area is very small, and conduction effects can be neglected. The approximate time is around 2 seconds.

The sum of the two mechanisms, determines the heat transfer of the sample in the system and knowing it the final temperature in function of time can be calculated, taking into account the initial temperature of the sample, because of the temperature dependence of different physical magnitudes involved in this thermodynamic study.

4.3.1.1 ANALYTICAL PROCEDURE FOR NATURAL CONVECTION

To solve the heat transfer equation, is needed to know the B value. This parameter includes the h value and to know it, previously the Grashof dimensionless number has to be calculated according to the equation:

$$Gr = \frac{g\beta\Delta TX^3}{\nu^2}$$

For this equation be assume that:

- $\beta = \frac{1}{T_f} = \frac{1}{294} [K^{-1}]$
- $X = \frac{L}{4} = \frac{50 \cdot 10^{-3}}{4} = 12.5 \cdot 10^{-3} [m]$
- ν : Kinematic viscosity is function of the temperature. As can be seen in the Annex1-Figure 13 according standard values, the evolution has been fitted to obtain an equation for a complete range of temperatures:

The obtained 4th polynomial fitted equation is:

$$y(x) = 4.565E^{-11}X^4 - 7.2098E^{-08}X^3 + 1.1138E^{-04}X^2 + 0.0865X + 13.318$$

(Values can be found in CD/CSTT/time-temp dependence.xls; sheet "kine visco AIR")

For each temperature, from -160°C to 20°C, fixing temperature increments with value of 10°C, and using the previous equation, Gr dimensionless number have been found.

Same procedure has been done to find the Prandtl dimensionless number (Pr), according to the equation:

$$Pr = \frac{\mu C_p}{k}$$

To obtain fitted values to determine, for each incremental step of temperature, the values of Cp and k (see CD/CSTT/Air K Fitting & Air Cp Fitting).

The obtained polynomial equations are:

$$C_p \rightarrow y(x) = 4.3207E^{-07}x^2 + 1.16296E^{-05}x + 1.00575$$

$$k \rightarrow y(x) = -2.72436E^{-05}x^2 + 0.07477x + 24.01686$$

(Values can be found in CD/CSTT/time-temp dependence.xls; sheets "Cp AIR" and "K Air" respectively and CD/CSTT/Cp Air Fitting)

Once Pr is obtained (see CD/CSTT/time-temp dependence.xls; sheet "Pr"), the product of Gr*Pr dimensionless numbers, is the Rayleigh dimensionless number which determine the type of flow regime.

As can be seen in CD/CSTT/time-temp dependence.xls; sheet "h Natural Conv f(T)" the maximum results is 1,112E+05, being less than 10⁹, concluding that in the case of the maximum difference between temperatures (-160°C to 21°C), the flow regime is laminar. The constants can be fixed, according standards, to calculate the Nu dimensionless number and finally obtain the h value for each incremental step of temperature.

Finally using the equation of the energetic balance, the B parameter is obtained, for each step. The Cp for X65 steel has been fitted (see CD/CSTT/time-temp dependence.xls; sheet "Cp Steel"), to obtain an equation to define its evolution in function of temperature (CD/CSTT/Cp Steel Fitting):

$$y = 0.44x + 450$$

Where: y represents Cp of the steel and x the temperature [J/KgK].

Fixing the initial temperature T_i , the final temperature in function of time can be determined. The results are plotted in the *Figure 4. 6*:

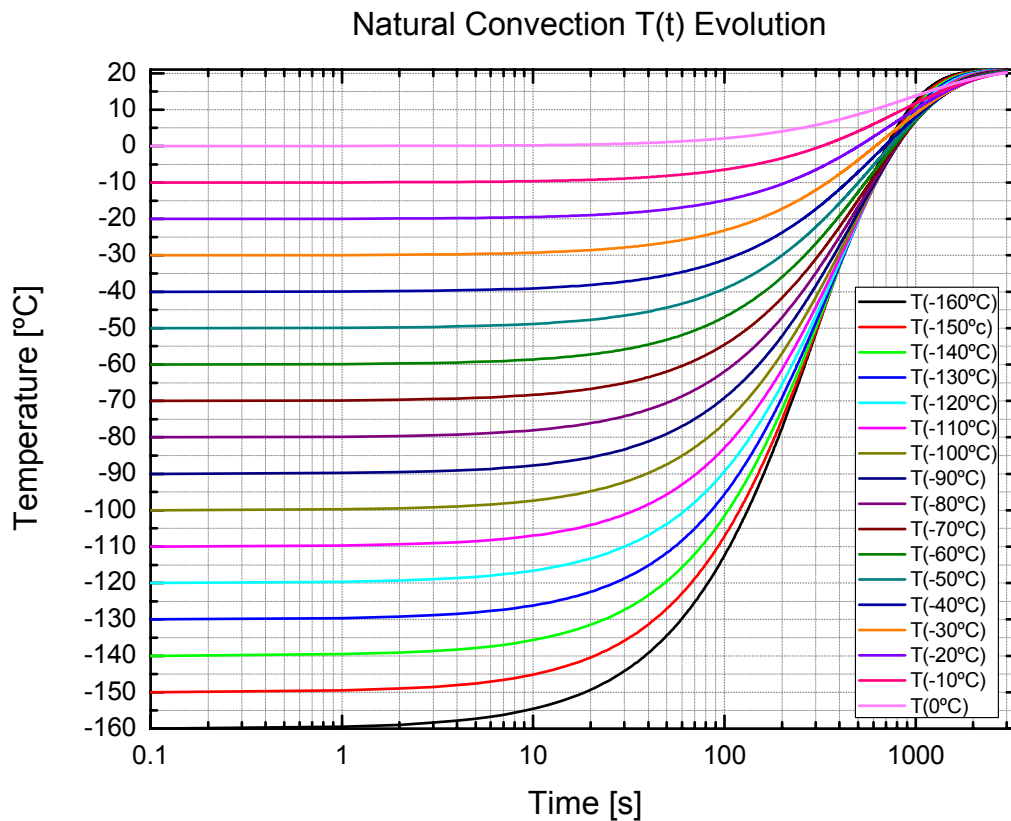


Fig. 4. 6 – Temperature evolution in function of time for each incremental step of temperature for natural convection

The main thermodynamics behaviors in case of natural convection that can be observed are:

- Long times are needed to reach the room temperature, so the heat transfer is very small because of h.
- In function of initial temperature, the temperature versus time evolution is different, however, in the initial times, from 0 to 20 seconds, the behavior is strongly similar in each initial temperature case.

In Figure 4. 7 the initial evolution is zoomed showing the temperature evolution of the sample:

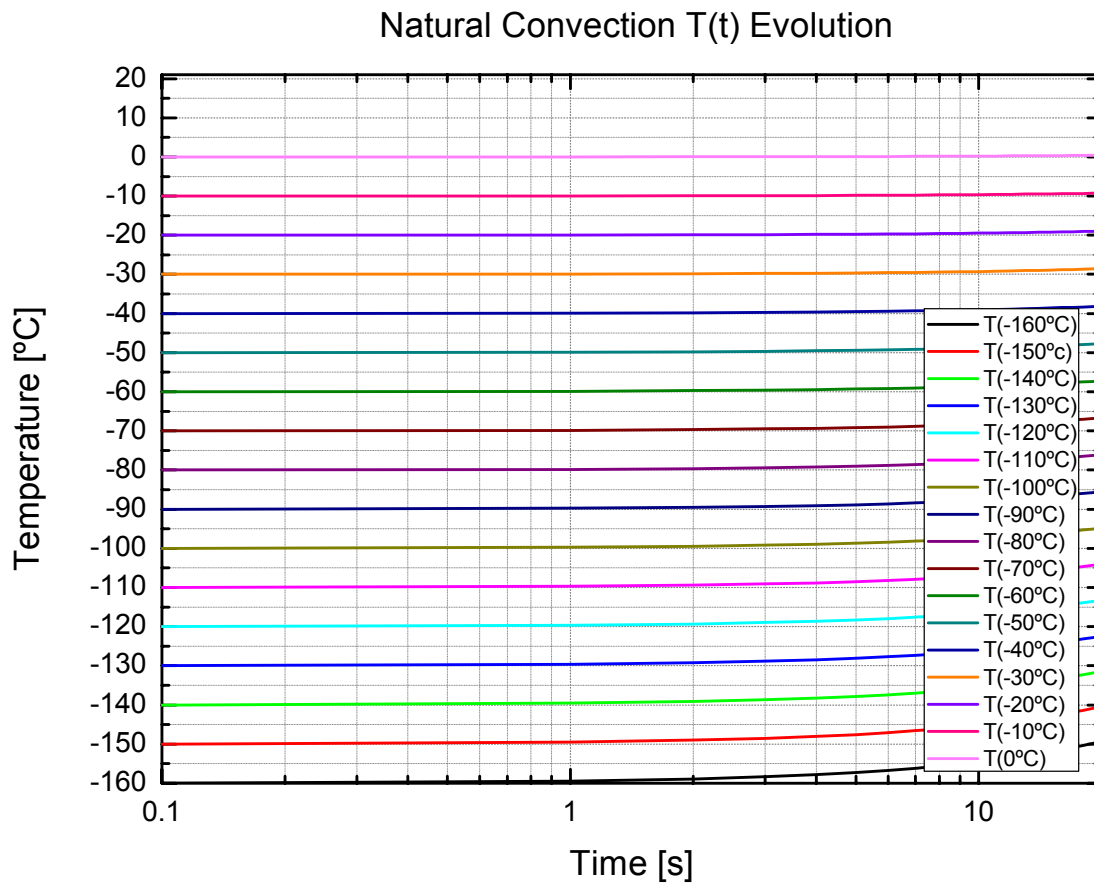


Fig. 4. 7 – Plotted zoom of temperature evolution for natural convection

4.3.1.2 ANALYTICAL PROCEDURE FOR FORCED CONVECTION

In case of forced convection, the same steps have been followed. In this case, but, the influence of the velocity is the main factor which permit increase the h value, and consequently the heat transfer in the system.

For this case, a velocity of 2.5m/s has been considered as the mean velocity required moving the sample from the fridge to the Charpy test machine, assuming that the velocity is not constant in all the procedure. This step needs around 5 seconds.

Using previous data fitted, when is required, the Re dimensionless number has been calculated for each increment of temperature (see CD/CSTT/time-temp dependence.xls; sheet "h Forced Conv f(T)").

Then considering a rectangular case and the flux situation as described in the *Figure 4. 8* for the cross section, the standard constants to be taken into account, can be seen below:

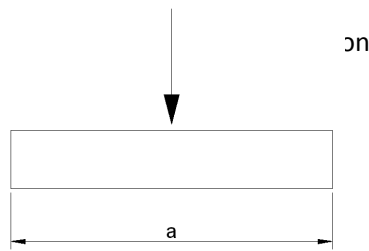


Fig. 4. 8 – Forced convection flux for rectangular cross section definition

- $C = 0.227$
- $m = 0.731$
- $X = \frac{2a}{\pi}$

As described previously and using the equation for cylinders of other cross sections different than circular cylinders, the Nu dimensionless number for each step of temperature have been found, and finally the h value for forced convective mechanism.

Fixing the initial temperature T_i , the final temperature in function of time can be determined, which results are plotted in the *Figure 4. 9*:

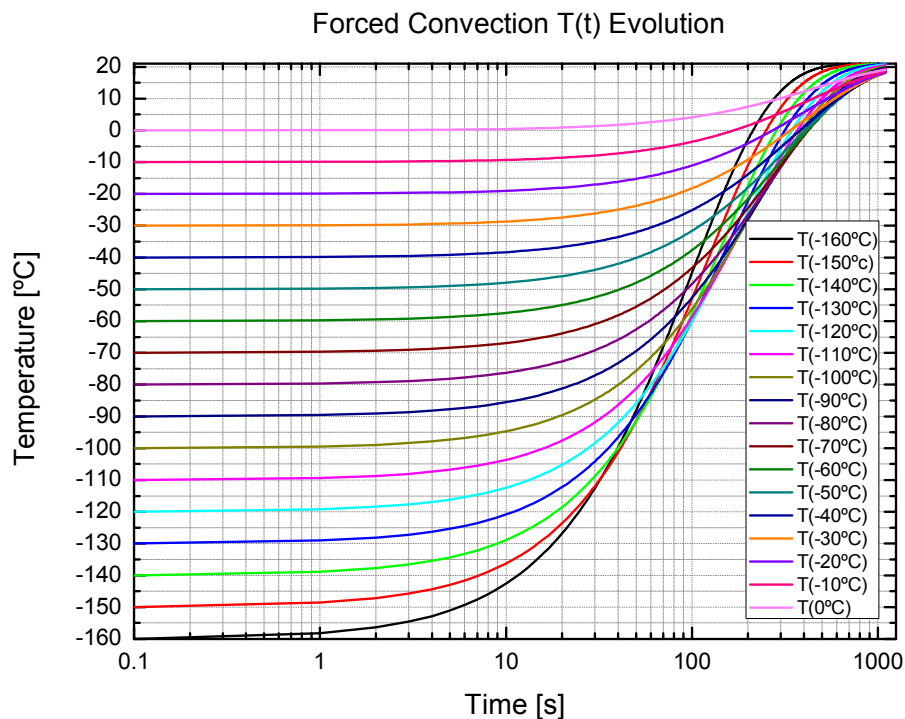


Fig. 4. 9 – Temperature evolution in function of time for each incremental step of temperature for forced convection

The main thermodynamics behaviors in case of forced convection that can be observed are:

- The times needed to reach the room temperature are quite lower than in natural convection. It can be deduced that the heat transfer is higher due the effects of the friction between fluid and the sample.
- In function of initial temperature, the temperature versus time evolution is different, in this case, in the graph appears different behaviors for each initial temperature.
- The initial time, is very important due that in few seconds, the heat transfer is very high, and the sample wins heat very fast from the air.

Figure 4. 10 shows the plotted graph zoomed in the initial times showing more clearly the temperature evolution of the sample in forced convection:

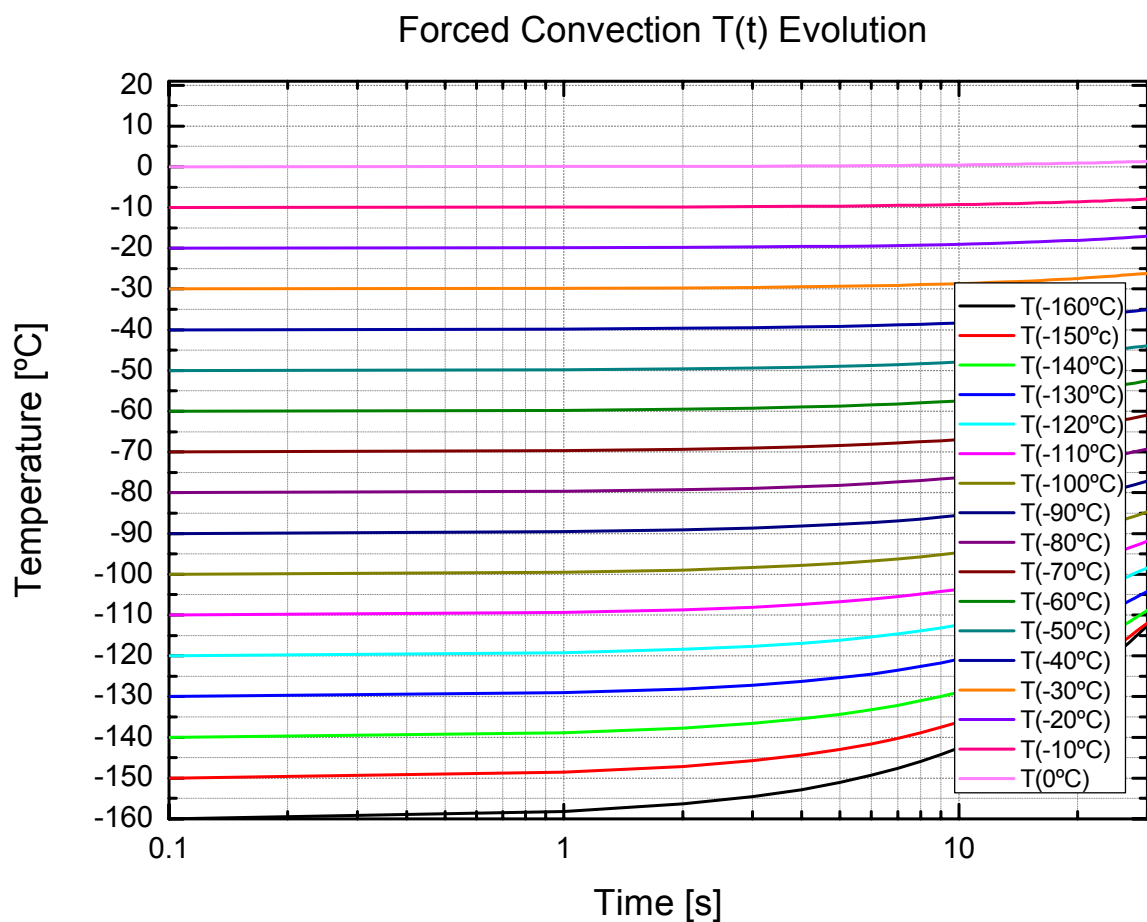


Fig. 4. 10 – Plotted zoom of temperature evolution in function of time for each incremental step of temperature for forced convection

4.3.2 EXPERIMENTAL PROCEDURE

Following, the temperature recorded temperature evolution is plotted (Figure 4. 11):

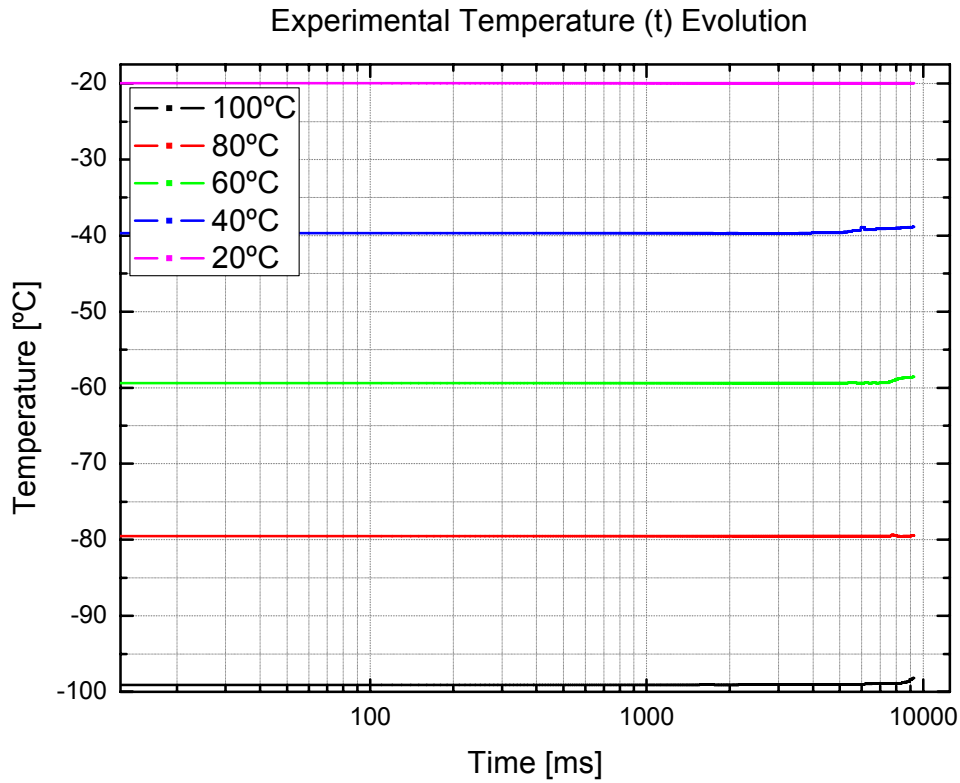


Fig. 4. 11 –Experimental Temperature vs. Time dummy evolution

Summarizing the recorded evolution of temperature in function of the time, as specified above, Table 4.4 shows the main important obtained data:

T[°C]	T1 (in freezer)[°C]	T2 (hit) [°C]	ΔT [°C]
-20	-19.9 ^{±0.1}	-19.1 ^{±0.1}	0.8 ^{±0.1}
-40	-39.7 ^{±0.1}	-38.7 ^{±0.1}	1.0 ^{±0.1}
-60	-59.4 ^{±0.1}	-58.1 ^{±0.1}	1.3 ^{±0.1}
-80	-79.5 ^{±0.1}	-78.0 ^{±0.1}	1.5 ^{±0.1}
-100	-99.0 ^{±0.1}	-97.2 ^{±0.1}	1.8 ^{±0.1}

Table 4. 4 - Recorded data summary

Where:

- T: Real temperature expected to reach.
- T1 : Real dummy temperature after 30 minutes.
- T2 : Real dummy temperature once the hammer impact.
- ΔT : Increment of temperature between T2-T1.

Comparing the values between experimental and theoretical model to predict the temperature values as appearing in *Table 4.5*:

T [°C]	$\Delta T_{NC(2s)}$ [°C]	$\Delta T_{FC(5s)}$ [°C]	Total ΔT [°C]	Diff[°C]	T _{model} [°C]	% Error
-20	0.1	0.5	0.6	-0.2	-19.39	-1.3 ^{±0.3}
-40	0.2	0.8	1.0	0.1	-38.96	-0.5 ^{±0.3}
-60	0.3	1.3	1.6	0.3	-58.42	-0.5 ^{±0.3}
-80	0.4	1.9	2.3	0.8	-77.72	0.4 ^{±0.3}
-100	0.5	2.7	3.2	1.4	-96.78	0.5 ^{±0.3}

Table 4. 5 - Validation summary

Where:

- T : Starting temperature test.
- ΔT_{NC} (2s): Increment of temperature by Natural Convection for last 2 seconds.
- ΔT_{FC} (5s): Increment of temperature by Forced Convection after 5 seconds.
- Total ΔT : Total increment of temperature in Charpy Test for 7 seconds.
- Diff : Difference of temperature between experimental and theoretical model.
- T_{model} : Final temperature predicted by the theoretical model.

It can be seen that the maximum error between the experimental temperature and the predicted temperature reach a maximum error value of 1.3^{±0.3}% when the dummy test is cooled at -20°C.

4.4 CHARPY V-NOTCH IMPACT TEST

The results of CVN tests are shown following (Figure 4. 12 until Figure 4. 15):

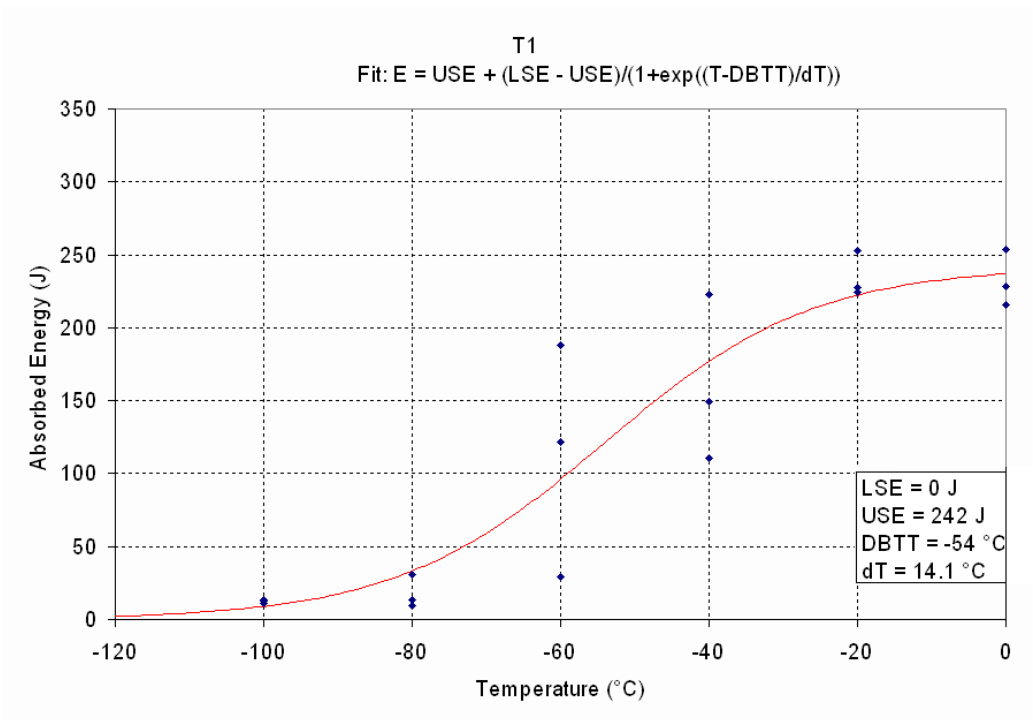


Fig. 4. 12 -T1 CVN Results

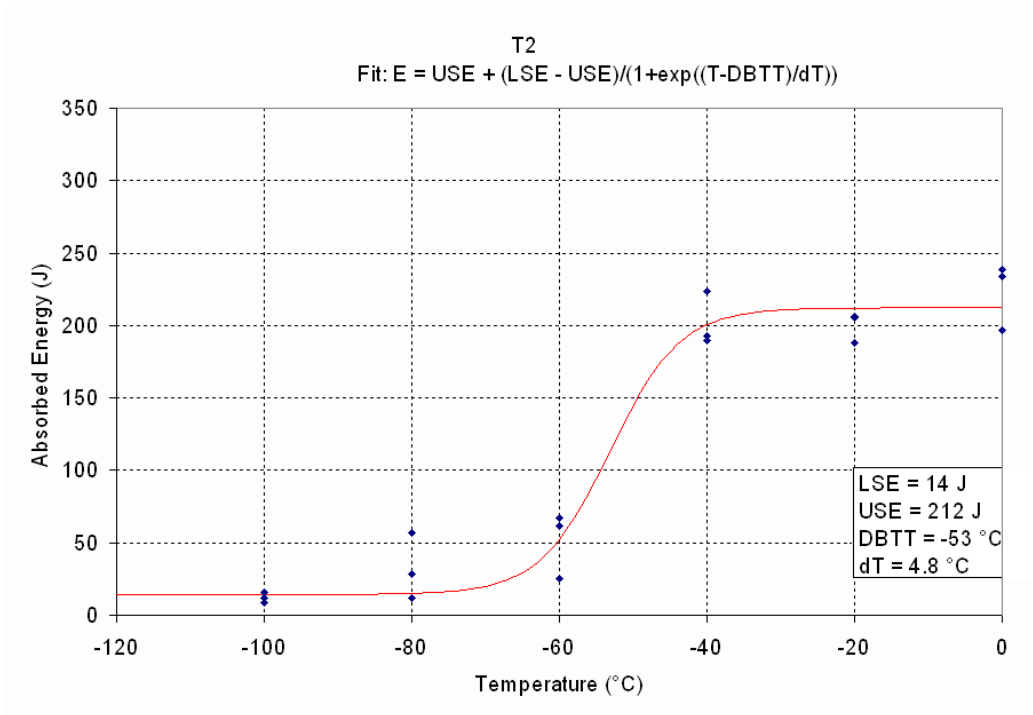


Fig. 4. 13 -T1 CVN Results

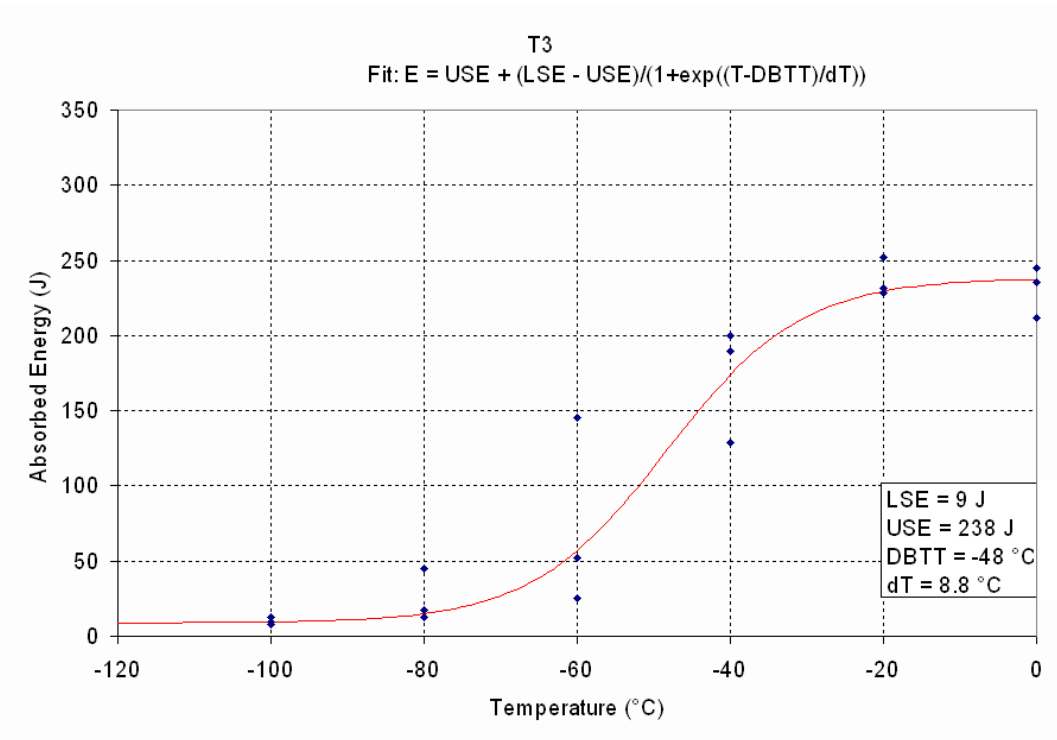


Fig. 4.14 -T3 CVN Results

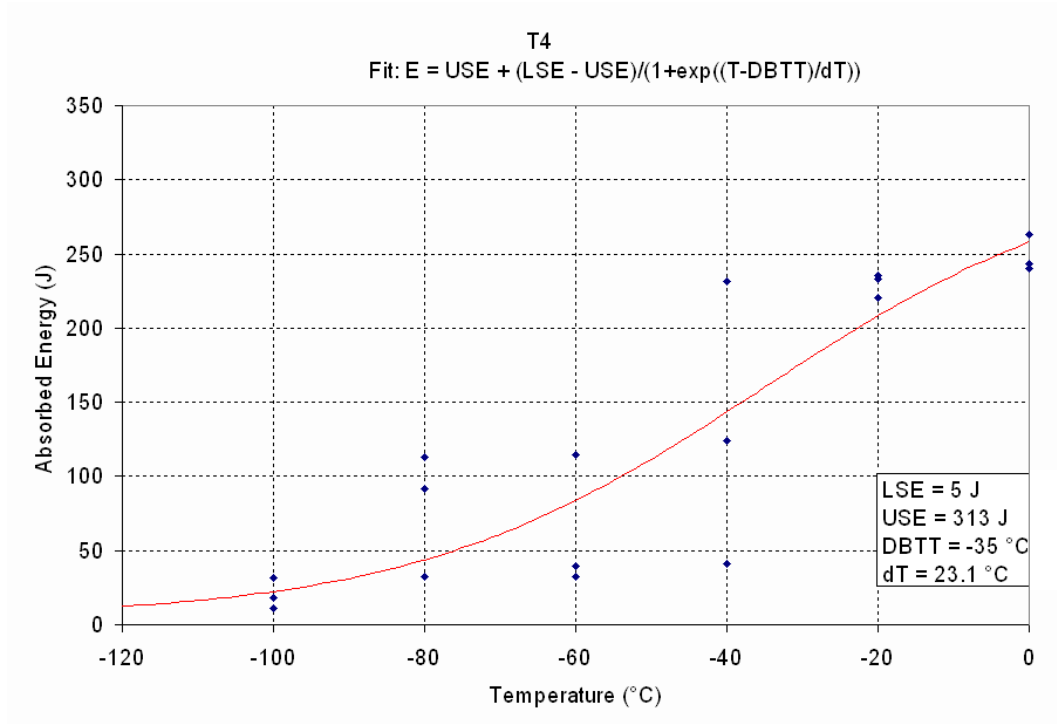


Fig. 4.15 -T1 CVN Results

Table 4.6 summarizes the main values obtained from CVN Impact test:

	T1	T2	T3	T4
USE [J]	242	212	238	313
LSE [J]	0	14	9	5
DBTT [°C]	-54	-53	-48	-35

Table 4. 6 – CVN Summarized Results

As can be observed in Table 4.6 the USE has a notably increase in T4 heated simulation. The rest of the heated simulations do not show any significant result of the ductility behavior of the material. It can be explained due the higher temperature and also higher time applied to the sample due to allow the material to unpin more dislocations and consequently the material can absorb more impact energy.

DBTT depends upon a number of factors, including the microstructure, the composition, the loading rate, and the test environment. The strain plays an important role one it, the higher the strain rate the higher the DBTT.

In this heated simulations, the temperature was below of recrystallization temperature, so no effects on strain can be expected, no changes in the dislocations global amount density. However, at higher temperatures and times, the unpinned number of dislocations is higher, than at lower temperatures and treatment times ($T1_{DBTT} = -54^{\circ}C$ and $T4_{DBTT} = -35^{\circ}C$).

4.5 FEM SIMULATION

POSTPROCESSING

As showed in *Figure 3.24* the last step once the FEM simulation is finished consists on the postprocessing analysis of the virtual obtained results.

Following the main steps of cold bending FEM simulation are showed (*Figure 4. 16 until Figure 4.18*):

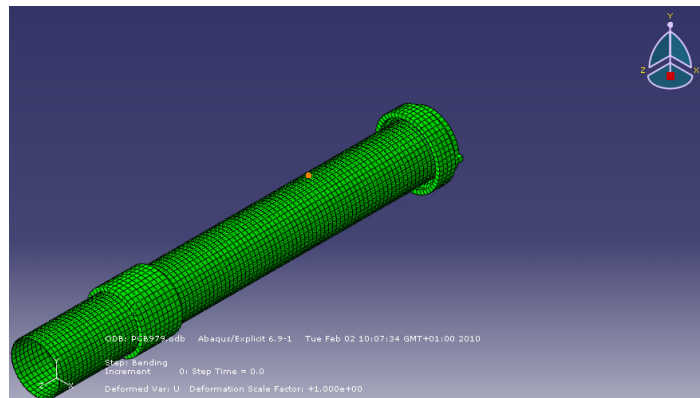


Fig. 4. 16 –Bending step at t=0s.

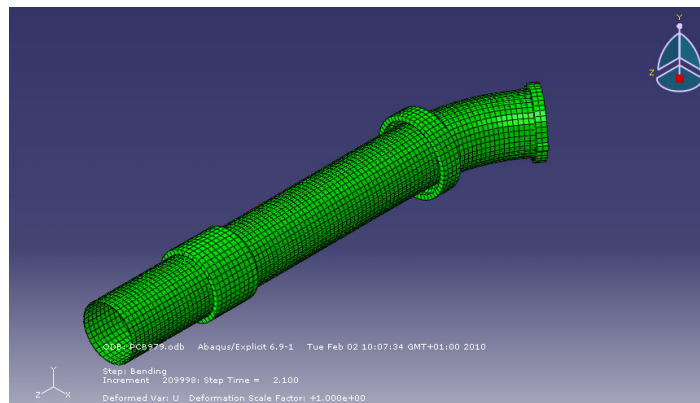


Fig. 4. 17 –Bending step at t=2.1s.

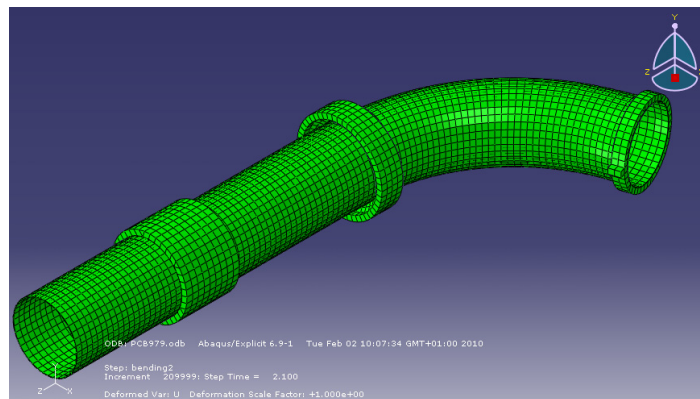


Fig. 4. 18 –Bending step finished.

Behavior Study of Pipes after Forming, Coating and Bending

It can be observed how the pipe is bended according the rotational movement described by the mobile clamp. The pusher helps the pipe to flow according rotational velocity and also avoid bending moments of the pipe tail.

The fixed clamp then, is the part when the pipe starts to bend remaining encastred during the whole simulation.

FEM software has different options to analyze the resultant simulated body. *Figure 4.19 & Figure 4.20* shows the Von-Misses stresses results:

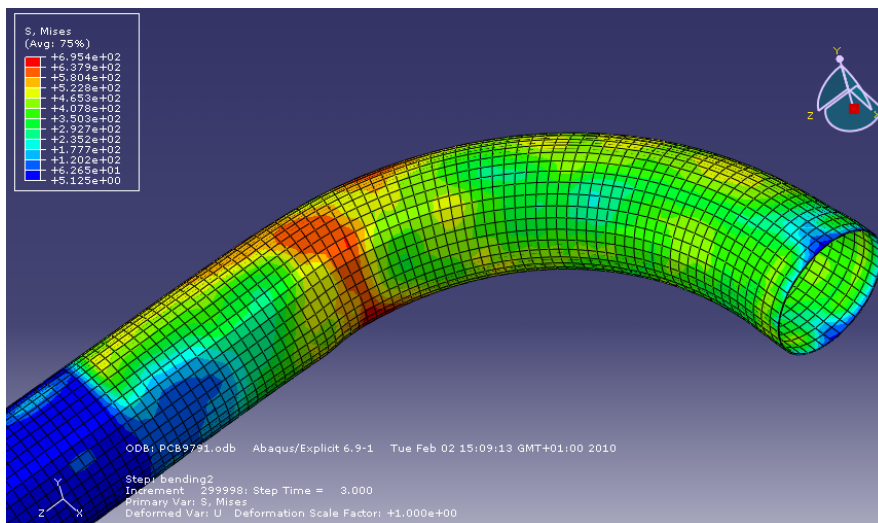


Fig. 4. 19 –Intradados Pipe Von-Misses Stresses

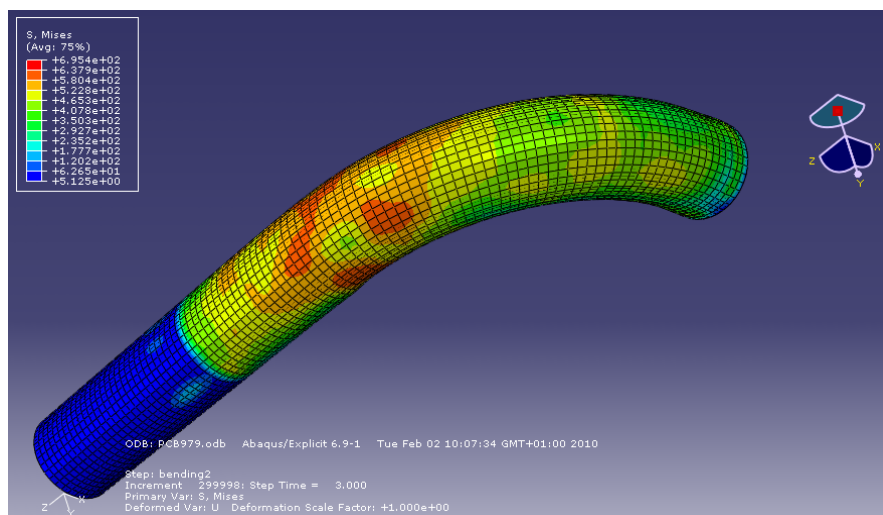


Fig. 4. 20 –Extradados Pipe Von-Misses Stresses

Pictures show stresses corresponding to the compression and tension stresses due the cold bending process.

From previous experimental test, same case was tested to know the mechanical properties of the material as can be seen in the following *Figure 4.21*. Using a software option “*query information at integration node*” Von-Misses stresses values from the FEM simulation can be known accurately in the same regions (*values obtained from the simulation are showed together with the Figure 4.21. Green boxes correspond to the cases that great accuracy within the results has obtained; Red boxes correspond to results with a discrepancy of ± 25 MPa that are assumed like bad results*):

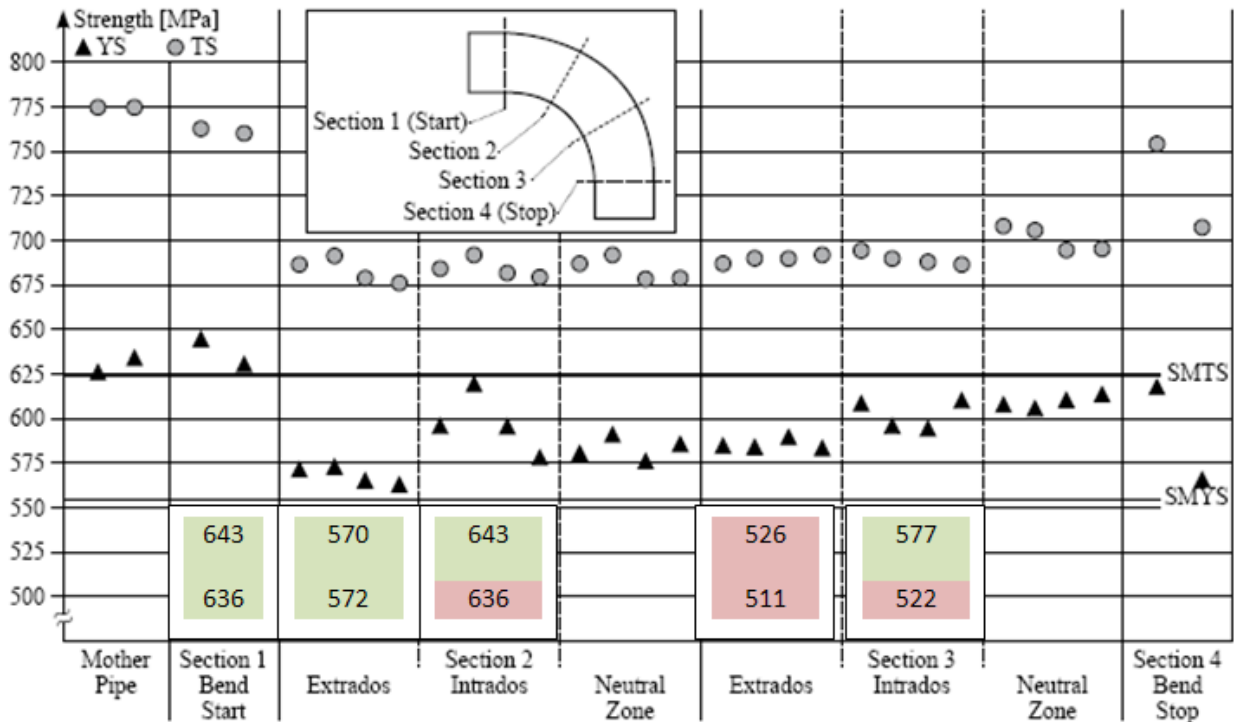


Fig. 4. 21 –Pipe Experimental Stresses and FEM Von-Misses Stresses

As can be seen, stresses values in section 1 and 2 are closed to the experimental values.

Closed to Section 3 the results show higher discrepancies, and section 4 due the use of not rigid tool to define the mobile clamp, the obtained results cannot be taking into account.

It can also be plotted the final strain state of the pipe after cold bending *Figure 4.22* and *Figure 4.23*:

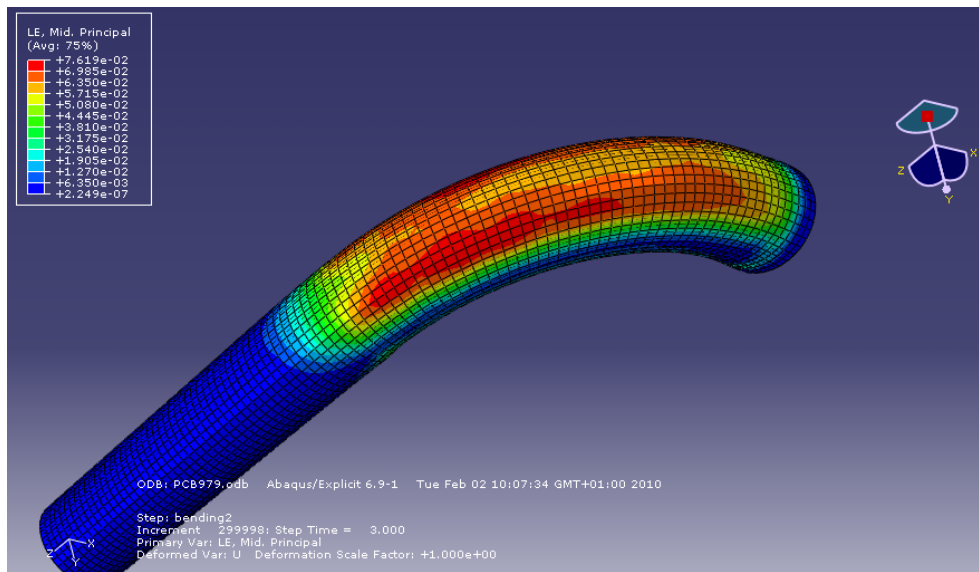


Fig. 4. 22 –Extrados Logarithmic Strain

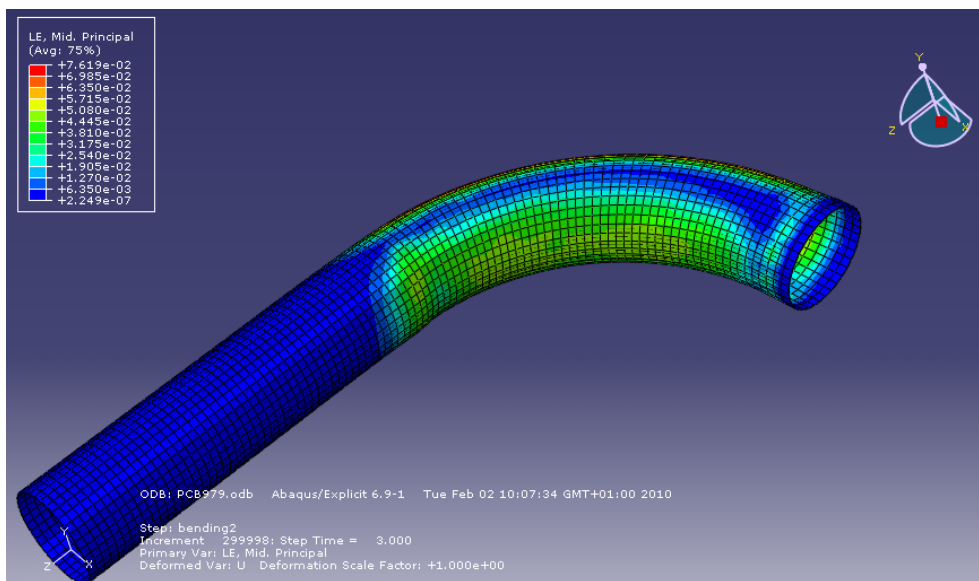


Fig. 4. 23 –Intrados Logarithmic Strain

The *Figure 4.22* shows higher strain values due the extension of the material (*extrados*). On the other hand *Figure 4.23* shows lower strain values in the compression zone (*intrados*).

Strain values cannot be contrasted neither previous FEM validated model nor experimental test.

5 CONCLUSIONS

The study of the coating processes has been done, and time and temperature range (minimum and maximum) has been also fixed.

Tensile tests have demonstrated that the UOE forming process, increase the strain in the pipe compared to base material. They also have showed the influence of strain in the mechanical properties of the x65 steel grade with and without the application of the coatings heated simulations, increasing the yield strength ($R_{p0.2}$) and reducing the rupture strain (A_{25}).

Charpy V-Notch impact tests have demonstrated the behaviour of the x65 steel grade with heated simulations under the application of dynamical loads showing how steel tends to increase the upper shelf energy (USE) and decrease the brittle-ductile temperature transition (BDTT), winning in ductility but losing however in the range of in service temperature.

Charpy V-Notch Samples Temperature Test have provide a better understanding of heat transfer in this type of steel, and a analytical procedure have been defined and parameterized in order to use with other steel data. This model has also been validated using experimental measurement and is helpfully in order to guarantee the quality of Charpy V-Notch experimental standards.

Finite Element Method (FEM) simulation of the cold bending pipe process have been done and also have been parameterized in order to be able to simulate different bending conditions changing some parameters such material, bending radius, thickness of the pipe, etc.

6 FUTURE WORKS

The effects of pre-strain in the base material need to be strongly considered due the direct impact on the mechanical properties in the pipelines steel grades.

Firstly, a better knowledge of the actual strain state of pipe circumferentially around itself has to be studied. After and once defined the actual strain ratios due the UOE forming process, a complete test program will include the application of strain into the samples from base material until strain % higher than the obtained in the pipe forming process.

All these samples will need to be heat treated more closely to the real process, in terms of heat application times.

All this tests can be carried out using the Gleeble simulator, a thermo-mechanical machine that can apply strain and controlled heated program.

Tensile and Charpy V-Notch tests will bring a deep knowledge of the mechanical properties of the steel due the coating recreations.

The FEM simulations need to be validated so experimental tests are required in order to ensure it. In other hand FEM simulations need to be coupled with the thermo-mechanical module to recreate and simulate the hot bending procedure.

Once the FM model will be validated, a parametric study will be carried out to predict the mechanical and/or thermo-mechanical behavior of the pipe under bending conditions in function of different parameters such: changes in thickness, in the material, in the heat treatment, in the bending radius.

7 ENVIRONMENTAL ASPECTS

The most remarkable environmental effect in the present project is the use of FEM simulation. Once the FEM model will be finished and validated, the final mechanical properties will be predicted. It means less amount of material, so can be translated directly into less contamination and energy save because of the less necessity to create the pipe and samples for testing.

8 COSTS

The costs of the present project have been divided in specific budgets:

BUDGET 1		CONCEPT: <i>FEM Software</i>			
REF.	DESIGNATION	UNIT	PRICE UNIT (€)	AMOUNT	TOTAL (€)
1.1	Abaqus [®] 6.9.1 License	Ut.	25.000	1	25.000
1.2	Abaqus [®] 6.9.1 Maintenance	Ut.	7.000	1	7.000
1.3	Computational equipment	Ut.	2.500	1	2.500
	- PC				
	- Operative System				
Total Budget:					34.500
Price Year Hour					3.93

BUDGET 2		CONCEPT: <i>Sample Preparation Machinery</i>			
REF.	DESIGNATION	UNIT	PRICE UNIT (€)	AMOUNT	TOTAL (€)
1.1	Drill	Ut.	40000	1	40000
Price Hour					22.7
1.2	Lathe	Ut.	28000	1	28000
Price Hour:					15.9

BUDGET 3		CONCEPT: <i>Staff</i>			
REF.	DESIGNATION	UNIT	PRICE UNIT (€)	AMOUNT	TOTAL (€)
1.1	Technician	Ut.	39000	1	39000
Price Hour					22.15
1.2	Research Engineer	Ut.	48250	1	48250
Price Hour:					27.41
1.3	Trainee	Ut.	7500 (6 Month)	1	7500
Price Hour:					8.52

BUDGET 4		CONCEPT: <i>FEM Simulation</i>			
REF.	DESIGNATION	UNIT	PRICE UNIT (€) ^{*1}	AMOUNT	TOTAL (€)
1.1	Preprocessing (Design and modelling)	h.	12.45	5	62.25
1.2	CPU Time (Solver calculation)	h.	12.45	6	74.7
1.3	Postprocessing	h.	12.45	1	12.45
Total Standard FEM Simulation Cost:					149.4
^{*1} Price unit includes: Price hour FEM simulations + Trainee Price Hour = 3.93 + 12.52 = 12.45€/h					

Behavior Study of Pipes after Forming, Coating and Bending

BUDGET 5		CONCEPT: <i>Tensile Samples and Test</i>			
REF.	DESIGNATION	UNIT	PRICE UNIT (€)	AMOUNT	TOTAL (€)
1.1	Tensile Samples Handling	h.	22.15	10	221.5
1.2	Machining : Lathe	h.	15.9	10	159
1.3	Test Machine	h.	20	12	240
1.4	Tensile Test Technician Services	h.	22.15	12	265.8
Total Tensile Samples and Test Cost:					886.3

BUDGET 6		CONCEPT: <i>CVN Samples and Test</i>			
REF.	DESIGNATION	UNIT	PRICE UNIT (€)	AMOUNT	TOTAL (€)
1.1	CVN Samples Handling	h.	22.15	70	1550.5
1.2	Machining : Drill	h.	22.7	70	1589
1.3	CVN Test Machine	h.	24	6	144
1.4	Tensile Test Technician Services	h.	22.15	11	243.65
1.5	Cryogenic Freezer Machine	h	21	11	231
Total Tensile Samples and Test Cost:					3758.15

BUDGET 7		CONCEPT: TOTAL PROJECT COSTS			
REF.	DESIGNATION	UNIT	PRICE UNIT (€)	AMOUNT	TOTAL (€)
1.1	FEM Simulation	Ut.	149.4	21	3137.4
1.2	Tensile Samples and Test	Ut.	1102.3	1	886.3
1.3	CVN Samples and Test	Ut.	3859	1	3758.15
1.4	Reading hours	h.	8.52	150	1022.34
1.5	Working Hours	h	8.52	750	6390
Total Project Costs:					15194.2

9 REFERENCES

- [1] - Guo B., Song S., Chacko J., Ghalambor A., *Offshore Pipelines*, Elsevier (2005).
- [2] - Mikael W. Braestrup, Jan Bohl Andersen, *Design and Installation of Marine Pipelines*, Blackwell Science Editorial 2005.
- [3] - Herynk M.D, Kyriakides S., Onoufriou A., Yun H.D., Effects of the UOE/UOC pipe manufacturing processes on pipe collapse pressure, *International Journal of Mechanical Science*, 533-553, (2007).
- [4] - Braestrup M.W, Andersen J.B, Andersen L.W., Bryndum M., Christensen C.J., Rishoj Nielsen N.J., *Design and installation of Marine Pipelines*, Blackwell Science (2005).
- [5] - Palmer A.C., King R.A, *Subsea Pipeline Engineering*, Pennwell Editorial 2004.
- [6] - American Petroleum Institute, *API 5L Specification for Line Pipe*, Exploration and Production Department (1995).
- [7] - Escoe A.K., *Piping and Pipeline Assessment Guide*, Elsevier (2006).
- [8] - *Standard Specification for Epoxy-Coated Steel Reinforcing Bars*, ASTM A 775/A 775M-97, American Society of Testing and Materials, 1997.
- [9] - Montalà F., *Materials selection and treatments*, EUETIT(2003).
- [10] - Dieter G.E., *Mechanical Behavior Under Tensile and Compressive Loads*, University of Maryland (1986)
- [11] - H.E. Davis, G.E. Troxell, and G.F.W. Hauck, *The Testing of Engineering Materials*, McGraw-Hill, New York (1964).
- [12] - J.M. Gere and S.P. Timoshenko, *Mechanics of Materials*, 4th ed., PWS Publishing Co., (1997).
- [13] - A.A. Griffith, *The Phenomena of Rupture and Flow in Solids*, Philos. Trans. Soc. (London) A, Vol 221 (1920).
- [14] - S.T. Rolfe and J.M. Barsom, *Fracture and Fatigue Control in Structures—Applications of Fracture Mechanics*, Prentice-Hall (1977).
- [15] - Holman J.P., *Heat transfers*, CECSA (1999).
- [16] - Cengel Y.A., *Heat Transfer a practical Approach*, Mc. Graw Hill (2003).
- [17] - Internal OCAS Project : OE0201020246 Charpy equipment; Number: 41783F2
- [18] - J.M. Barsom, *Effect of Temperature and Rate of Loading on the Fracture Behavior of Various Steels, Dynamic Fracture Toughness*, The Welding Institute (1976).
- [19] - Users Abaqus® 6.9.1 Theory Manual, Simulia (2009).
- [20] - Source: “ Fabrication of hot induction bends from LSAW large diameter pipes manufactured from TMCP plate”; *Microalloyed Steels for the Oil & Gas Industry International Symposium*; January 22-27, 2006
- [21] - Source: “First x80 Pipeline section in Italy”; *PRCI/EPRG/APIA, Technical Conference* May 15-20, 2005 Orlando-USA; Europipe.

ABSTRACT

A study of the main types of coatings and its processes that modern industry commonly apply to prevent to the corrosion due to the environmental effects to energetic market pipelines have been done.

Extracting main time and temperature range values, coating heat treatment recreation have been applied to x65 pipelines steel grade samples obtained from a pipe which was formed using UOE forming process.

Experimental tensile tests and Charpy V-Notch Impact test have been carried out for a deeply knowledge of the influence on the steel once this recreations are applied. The Yield Strength and toughness have been improved despite lower values in rupture strain and ductile-brittle temperature transition have been obtained.

Finite Element Method have been applied to simulate the entirely pipe cold bending process to predict the mechanical properties and behaviour of the pipe made from x65 steel grade under different conditions.

RESUM

L'estudi dels tipus de recobriments y processos principals que la industria moderna actual aplica per tal de prevenir la corrosió degut als efectes mediambientals sobre les tuberies usades en el sector energètic ha sigut realitzat.

Extraient els principals rangs de valors de temps i temperatura, la recreació dels tractaments tèrmics dels processos de recobriment han sigut aplicats sobre acer de tuberies x65 obtingut d'una tuberia fabricada utilitzant el procés UOE de fabricació.

Tests experimentals de tracció i d'impacte Charpy amb entalla en V han sigut realitzats per tal d'obtenir un profund coneixement de la seva influencia en l'acer un cop aplicats aquests tractaments tèrmics. El límit elàstic i la tenacitat han sigut millorades malgrat valors més baixos de deformació última i de temperatura de transició fragil-dúctil han sigut obtinguts.

Mètodes d'elements Finitos han sigut aplicats per tal de simular el procés complet de flexió en fred de tuberies per tal de predir les propietats mecàniques finals així com el comportament de la tuberia feta d'acer x65 sota diferents condicions.